

The Geology and Geography of Floods

Jim E. O'Connor

U.S. Geological Survey, Portland, Oregon

Gordon E. Grant

U.S. Forest Service, Corvallis, Oregon

John E. Costa

U.S. Geological Survey, Portland, Oregon

From a global perspective, the magnitude, duration, and volume of riverine floods vary widely depending on source mechanism, global location, geology, and physiography. But despite this variance, there are real physical limits as to how large a flood can be. Meteorological floods result from individual storms of various types that deliver water volumes as great as 10^{11} m³ over a few days or weeks as well as from seasonally persistent climate patterns that deliver upwards of 10^{12} m³ over several weeks or months and cause peak discharges of as much as 10^5 m³/s within large, continental-scale basins. The fundamental limits to meteorologic flooding depend primarily on precipitation rates and volumes, and the efficiency with which distributed rainfall concentrates into channel networks. Global and U.S. flood records show that for basins primarily affected by individual storms, the largest flows are in areas where atmospheric moisture or storm tracks are intercepted by local topographic relief. For larger basins, the largest flows result from seasonally persistent climate patterns and, on a global basis, are generally in the tropical regions where there is more precipitable moisture. Especially notable is the contribution of high-relief topography to meteorologic flooding because of its double effect of (1) lifting of atmospheric moisture, thus increasing local precipitation, and (2) promoting faster concentration of flow into channels. Floods from dam failures and terrestrial freshwater sources such as lakes and ice caps involve similar total volumes as meteorological floods, up to 10^{13} m³, but with much larger discharges—as great as $2 \cdot 10^7$ m³/s. The largest well-documented dam-failure floods have been during Pleistocene ice ages when glaciers and changing hydrologic conditions deranged drainage systems, causing large lakes to breach ice dams and basin divides. The

largest historic floods from terrestrial water sources have had discharges as great as $1.5 \cdot 10^6 \text{ m}^3/\text{s}$ and include floods from volcanic-induced melting of ice caps and failures of ice and landslide dams. The fundamental limits to dam-failure floods primarily arise from the size of the outlet channel and the volume of the impounded waterbody.

INTRODUCTION

Riverine floods come in a wide range of frequencies and magnitudes from various geophysical mechanisms. Viewed over geologic time and space scales, however, fundamental climatologic, topographic, and geologic factors substantially influence and limit local flood volumes and magnitudes in predictable ways. Many of these influences are obvious, such as the relationship of certain types of floods to local topographic and climate patterns. But some are less obvious, including geologic controls on the timing, location, and magnitude of natural dam failures. In this paper, we outline some of the primary factors that influence the magnitude of floods and how these factors vary temporally and spatially over geologic time and space scales.

Our motivation is the perception that the human perspective of floods is often narrow, usually focusing on experiences or hazards of floods on particular rivers. Even seasoned hydrologists and geologists treat floods outside of modern experience, such as the great Pleistocene Missoula Floods, as scientific curiosities. Such great floods are intrinsically interesting because of their perceived uniqueness and dramatic role in shaping the landscape, and have served as lightning rods for inquiry and controversy, but they are not usually considered as a component of normal geophysical behavior. But indeed floods of all sizes and sources can be viewed as a geologic process on par with other Earth-system processes, such as tectonics and atmospheric circulation, with attributes, causes, effects, and even interrelationships that span similar ranges of scale.

Practitioners of paleoflood hydrology [*Kochel and Baker, 1982*], who study floods of all scales and from many different geologic eras and environments, are well situated to appreciate, describe, and even quantify these interrelationships. Indeed, many of the papers in this volume provide examples of floods resulting from these geologic, physiographic, and climatologic interactions in specific settings. The purpose of this paper is to provide an overall context for these individual paleoflood studies by systematically describing spatial and temporal distribution of large floods and flood-generating mechanisms, thereby establishing a framework for the environmental setting of floods over Earth history. These results are consistent with physical limits for terrestrial floods determined from general consideration of flood generation processes.

What is a flood? Simply stated by a prominent geomorphologist and hydrologist: "Floods come from too much water" [*M.G. Wolman, pers. comm., 1983*]. For the purposes of this paper, we consider floods as notable flows of channelized water. In other words, there are no specific criteria that we are using to define a flood. Many of the floods that we describe or include in our analyses were damaging and geomorphically effective, but our discussion is not limited to such events. Nor do we rely on other measures of flow magnitude such as recurrence interval or the relation of flow stage to channel banks or floodplain elevations. Such measures are either difficult to characterize or irrelevant for floods of diverse origins and scales. Our discussion is restricted to riverine floods, so we are excluding flooding of shorelines associated with rising lake or sea levels.

This paper is organized by the following five premises, each of which builds upon the previous one and is elaborated in the following sections with data compilations and specific examples.

1. Floods are the product of the release of stored water into channels and floodplains.
2. The magnitude of floods depends on storage, release, and transfer processes and rates.
3. Certain geologic, climatologic, and physiographic settings result in storage volumes and release rates that produce larger floods than in other settings.
4. These large-flood settings are generally predictable within an overall geologic and geographic framework.
5. Observations of flood magnitude, duration, and volume are consistent with global physical limits to flooding that result from factors such as topography, rainfall rates, and basic hydraulic principles.

STORAGE RESERVOIRS AND RELEASE MECHANISMS

All floods result from the rapid release of water onto the landscape. The geography of floods is therefore closely tied to those parts of the Earth where large quantities of water can both accumulate and be released quickly to channels and floodplains. Water can be stored both in the atmosphere as vapor, or terrestrially as liquid water or solid ice and snow. Both atmospheric and terrestrial sources of floods have characteristic volumes and release rates that affect

Table 1. Global freshwater budget (from Barry and Chorley, 1992).

Location	Source	Percent
Terrestrial	Ice Sheets and Glaciers	74.6
	Ground water	25.0
	Lakes	0.3
	Soil Moisture	0.06
	Rivers	0.03
Atmosphere	Precipitable Moisture	0.035

their potential to cause large flows. The non-uniform and non-random geographic distribution of these flood-generating sources and processes means that the potential for large floods is concentrated in specific arrangements of physiographic and atmospheric features. In this section we review atmospheric and terrestrial water sources, including their areal extents and volumes, geographic distribution, and rates and mechanisms of release.

Global Water Storage

Most of the Earth's water (97%) is stored in the oceans [More, 1967]. Of the world's fresh water (3% of total), almost 75% is frozen for centennial to millennial timescales in ice sheets and glaciers (Table 1). Virtually all remaining fresh water is stored as groundwater. All water readily available to cause floods—that is water stored as lakes, rivers, soil moisture and the atmosphere—accounts for only 0.4% of total fresh water and 0.01% of global water volume. The amount of water vapor stored in the atmosphere, expressed as average depth over the Earth's surface, is only 2.5 cm [Barry and Chorley, 1992].

Atmospheric Storage and Delivery

Despite this almost minuscule amount of atmospheric water storage relative to the total volume of water on Earth, under the proper conditions huge fluxes of moisture can be concentrated and delivered to the landscape, either in individual storms or from persistent patterns of weather or climate (Figure 1, also on CD). For individual storms, these conditions depend primarily on micro- to macro-scale vertical and, to lesser extent, horizontal motions of the atmosphere that cause moisture-laden air to converge and accumulate. At time scales greater than a few days or weeks, synoptic and global patterns of horizontal atmospheric motion control rates and volumes of precipitation delivery [Hayden, 1988].

Individual storms. As summarized by Hirschboeck [1991], individual storms precipitate moisture because of

air-mass uplift and consequent cooling and release of water as rain or snow. Such air-mass uplift generally results from: (1) thermal convection, (2) large-scale frontal convergence of warm and cold air masses, (3) upper air disturbances, and (4) orographic lifting. Convective processes include thunderstorms, tropical and extratropical cyclones, and mesoscale convective complexes or systems. These span a wide range of spatial scales, from 10^1 to 10^2 km² for individual thunderstorms, to thunderstorm systems (mesoscale convective complexes) spanning 10^3 to 10^5 km², to hurricanes that can cover 10^6 km² or more. Such convective systems can produce extremely intense precipitation, leading to flash floods in small watersheds or regional floods in larger basins. Frontal convergence occurs over large (10^5 to 10^6 km²) areas, leading to large basin floods. Upper air disturbances and orographic lifting can occur over small or large areas and have similarly local or widespread effects on flooding.

Storm systems can be thought of as moisture reservoirs, with permeable and often ill-defined boundaries, but distinctive spatial and temporal scales. Of specific importance to flooding is the volume of water stored in and delivered by these types of storm systems and delivery processes. There have been few systematic studies to compare storms of different types in terms of their total moisture volumes. Storm systems are typically described in terms of total precipitable water [e.g. Bradley and Smith, 1994]: the liquid equivalent of water vapor in an atmospheric column or from the surface to a specified barometric surface (i.e., 300 mb). For example, Bradley and Smith reported that total precipitable water from 33 extreme rainstorms in the southern U.S. ranged from 26.4 to 56.1 mm. For storms where the precipitable water content is known, the entire storm system can be considered an atmospheric source, with the total volume of water available for runoff being the product of the precipitable water and the areal extent of the storm system. For the more typical case in which areal extent and total precipitable water are not reported, we can approximately calculate the total storage volume as the product of storm area, average rainfall intensity, and storm duration. Representative values of these parameters for various storm types as reported in the meteorological literature are shown in Table 2. Total storm volumes range from $1.8 \cdot 10^5$ to $2.1 \cdot 10^7$ m³ of water for small and intense convective cells to $6.1 \cdot 10^9$ m³ for mesoscale convective complexes to $4.7 \cdot 10^{10}$ m³ for hurricanes.

Rainfall volumes from individual storms can also be estimated from measurements of precipitation depth, area, and duration for individual storms (Figure 2, also on CD). For example, Leopold [1942] summarized such data for six convective summer thunderstorms in Arizona and New

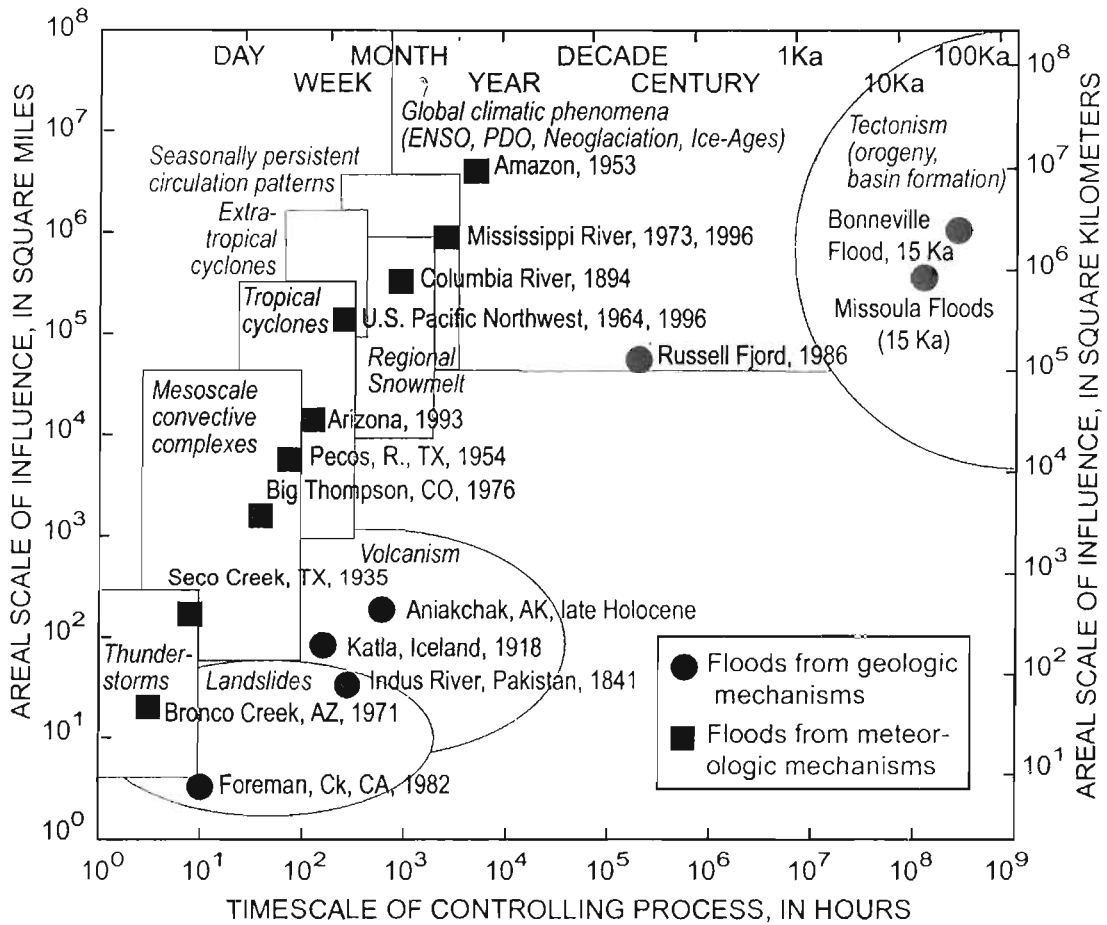


Figure 1. Space-time domain for selected meteorologic and geologic processes that can cause floods. Selected floods also shown. After Hirschboeck (1988).

Mexico, for which total rainfall exceeded volumes ranging between $6.5 \cdot 10^5$ and $4 \cdot 10^7$ m³. The *World Meteorological Organization* [1986, p. 261-263] has compiled observations of maximum depth-area-duration for individual storms (Figure 2b), for which the largest measured rainfall volume resulted from a 1916 hurricane centered in Florida that delivered an average of 226 mm of rainfall over 260,000 km², for a total of $6 \cdot 10^{10}$ m³ of water. Similarly, $4.3 \cdot 10^{10}$ m³ of water was precipitated by a 1967 hurricane in Texas. The thunderstorm that produced the record 4.5-hour rainfall at Smethport, Pennsylvania, during July 17-18, 1942 (Figure 2a) had a total storm volume in excess of $2.7 \cdot 10^9$ m³. Exceptionally large and wet hurricanes not included in the World Meteorological Organization database likely produced even more precipitation. For example, maps of total precipitation resulting from the Oct.-Nov. 1998 Hurricane Mitch in Central America (<http://cindi.usgs.gov/hazard/event/mitch/mitch/atlas/hmprecip.html>; May 25, 2001) indicate a total precipitation volume of about $2 \cdot 10^{11}$ m³.

Persistent patterns of moisture delivery. Floods in larger basins more typically result from persistent precipitation-enhancing synoptic weather or climate. Precipitation is still delivered by individual storms or convective cells as described in the previous section, but the frequency, intensity, and duration of such storms can be affected by regional or global atmospheric patterns that can persist for months to decades. Such patterns include quasi-stationary trough-and-ridge patterns of upper atmospheric circulation that can promote continued atmospheric convergence over areas of 10^5 to 10^7 km² for several days or weeks. Such a condition over the north-central United States was the cause of the Mississippi River floods of 1973 and 1993 [Hirschboeck, 1991; 2000]. Climatic conditions of annual to decadal duration that can cause regionally enhanced precipitation include coupled atmospheric and oceanic phenomena of hemispheric or global scales such as the El Niño/Southern oscillation (ENSO) and the Pacific Decadal Oscillation (PDO; e.g. *Cayan and Peterson, 1989; Dettinger and Cayan, 2000*). Even longer-term climate fluctuations,

Table 2. Selected estimates of precipitation volume for representative storm types.

Storm type	Area (km ²)	Duration (hrs)	Peak intensity (mm/hr)	Total volume precipitated (m ³ ·10 ⁶)	Reference
Small convective cell (intense phase) ^a	25	0.5		21.6	Ludlam, 1980 (p. 271)
Large cumulonimbus convection cell	32,400	20	90.0	450 ^b	Ludlam, 1980 (p. 298-299)
Mesoscale convective complex	82,000	24	6.8	6,100 ^c	Cotton and Anthes, 1989
Hurricane (avg)	31,000	72 ^d	21.0	47,000	

^a Average precipitation for storms with and without hail
^b Total storm volume quoted as 4.5·10¹² kg over an area of 32,400 km²
^c From time-averaged integral of 82 storms
^d Assumes a 200-km inner-area diameter
^e Assumes 3-day duration

such as century- and millennial-scale periods of global cooling and warming (e.g. the Neoglacial Period, Medieval Optimum, and Pleistocene ice ages), may be relevant to flood frequency and magnitude [e.g. Ely et al., 1993].

It is more difficult to determine directly the volumes of water delivered by persistent climate and weather regimes. Indirect minimum estimates can be obtained by considering the size of floods that have resulted from periods of enhanced precipitation, although this substantially underestimates total volumes by not accounting for water lost to evapotranspiration or long-term ground-water storage. Nevertheless, some values that may be representative include 4.9·10¹¹ m³ of water for the 1973 flood on the Mississippi River and 4·10¹² m³ for the 1953 flood on the Amazon River in Brazil (Table 3). These values suggest that persistent weather and climate patterns over large basins can produce water volumes several times greater than the wettest individual storms (Table 2).

Rates of atmospheric moisture delivery. A primary factor controlling the discharge of meteorological floods regardless of atmospheric source is the rate of transfer of water from atmospheric storage to the landscape by precipitation. Record rainfall amounts vary from 38 mm in 1 minute at Barot, Guadeloupe (West Indies), to over 40 m during 2 years of strong monsoon circulation at Cherranpunji, India (Figure 2a). In spite of the broad range of volumes of water delivered by various types of storm systems and persistent weather patterns, maximum rainfall intensities follow a well-defined relationship.

$$P = 350D^{0.49} \quad (r^2=0.99), \quad (1)$$

over six orders of magnitude, where P equals maximum observed precipitation depths in millimeters and D is duration in hours (Figure 2a). Although there are no

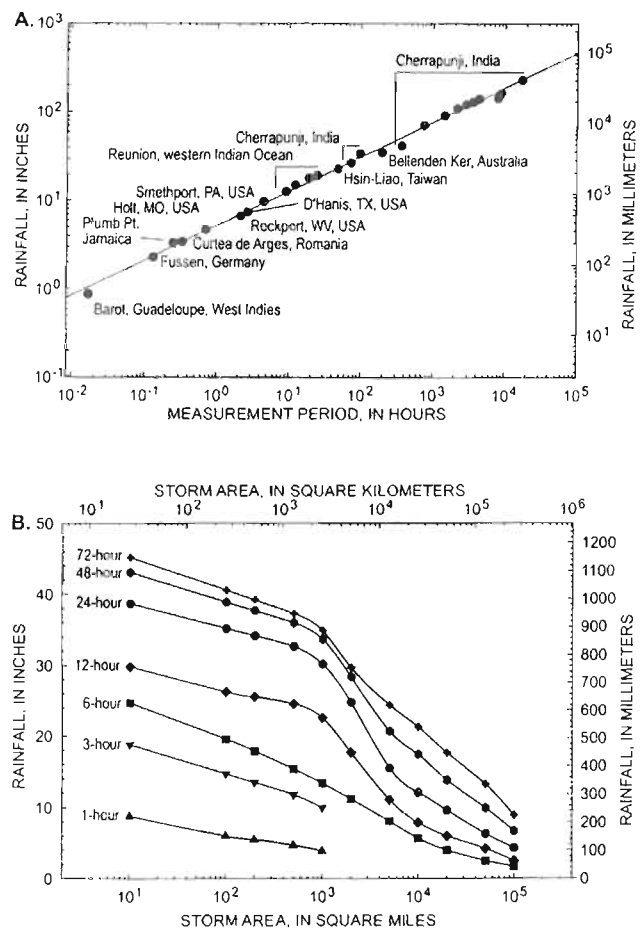


Figure 2. Maximum rainfall observations. A) Global maximum point rainfall measurements for various time intervals. Data from *World Meteorological Organization*, 1986, p. 258. B) Maximum depth-area-duration precipitation measurements for U.S. storms. Data from *World Meteorological Organization*, 1986, p. 261.

Table 3. Selected floods from natural dam failures, constructed dam failures, and meteorological events (“–” indicates no data; “n.a.” indicates “not applicable.”)

River/dam-/lake	Location	Date of Flood	Type of Dam or Flood	Dam Height (m)	Breach Depth (m)	Volume (m ³)	Peak Discharge (m ³ /s)	Duration ^a (hours)	Reference
Natural dams failures									
Kuray	Altai, Russia	Pleistocene	Glacier	--	900	1.0·10 ¹²	1.8·10 ⁷	3.1·10 ¹	Baker et al., 1993
Lake Missoula	Montana, US	Pleistocene	Glacier	--	525	2.2·10 ¹²	1.7·10 ⁷	7.2·10 ¹	O'Connor and Baker, 1992
Lake Bonneville	Idaho, US	Pleistocene	Basin sill	280	108	4.8·10 ¹²	1.0·10 ⁶	2.6·10 ³	O'Connor, 1993
Aniakchak River	Alaska, US	Holocene	Caldera	183	183	3.7·10 ⁹	1.0·10 ⁶	2.1·10 ⁰	Waythomas et al., 1996
Columbia River	Oregon, US	Holocene	Landslide	75	60	2.1·10 ¹⁰	2.2·10 ⁵	5.3·10 ¹	O'Connor et al., 1996
Russell Fiord	Alaska, US	Oct. 8, 1986	Glacier	25.5	25.5	5.4·10 ⁹	1.1·10 ⁵	2.9·10 ¹	Mayo, 1989
Indus River	Pakistan	June, 1841	Landslide	150	150	1.2·10 ⁹	5.7·10 ⁴	1.2·10 ¹	Hewitt, 1968; Shroder et al., 1991
Rio Mantaro	Peru	Oct. 28, 1945	Landslide	96.3	55.8	3.0·10 ⁸	1.2·10 ⁴	1.4·10 ¹	Snow, 1964
Rio San Pedro	Chile	July 25, 1960	Landslide	--	43	2.0·10 ⁹	7.5·10 ³	1.5·10 ²	Pena and KJohn, 1989
Lag. Jancaruish	Peru	Oct. 20, 1960	Moraine	21	21	8.0·10 ⁶	7.5·10 ³	5.9·10 ¹	Lliboutry et al., 1977
Lag. Josefina	Ecuador	May 10, 1993	Landslide	80	40	1.2·10 ⁸	5.0·10 ³	1.3·10 ¹	Zevallos-Moreno, writ. comm., 1993
Isfayramsay R.	Russia	June 18, 1966	Landslide	90	90	6.5·10 ⁸	5.0·10 ³	7.3·10 ¹	Glazyrin and Reyzvikh, 1968
Lake Nostetuko	Canada	July 19, 1983	Moraine	--	38.4	6.5·10 ⁶	5.7·10 ²	6.3·10 ⁰	Blown and Church, 1985; Clague and Evans, 1994
Rio Pisque	Ecuador	Jan. 26, 1990	Landslide	45	30	2.5·10 ⁶	4.8·10 ²	2.9·10 ⁰	Plaza-Nieto et al., 1990; Zev.-Mor., w. comm., 1993
N. Fork Toutle R.	Wash., US	Aug. 27, 1980	Landslide	9	9	3.1·10 ⁵	4.5·10 ²	3.8·10 ¹	Jennings et al., 1981; Costa and Schuster, 1991
Rio Toro	Costa Rica	July 13, 1992	Landslide	52	50	5.0·10 ³	4.0·10 ²	6.9·10 ¹	Mora et al., 1993
Squaw Creek	Oregon, US	Sept 7, 1970	Moraine	22.4	22.4	3.2·10 ⁵	2.8·10 ²	6.3·10 ¹	O'Connor et al., in press
Tunawaea R.iver	New Zealand	July 22, 1992	Landslide	50	20	6.3·10 ⁵	2.5·10 ²	1.4·10 ⁰	Jennings et al., 1993
Constructed dam failures									
Teton	Idaho, US	June 5, 1976	Earthen	93	67	3.1·10 ⁸	6.5·10 ⁴	2.6·10 ⁰	Costa, 1988; MacDonald and Langridge-Monopolis 1984;
Malpasset	France	Dec. 2, 1959	Masonry	61	61	2.2·10 ⁷	2.8·10 ⁴	4.3·10 ¹	Costa, 1988
St. Francis	Calif., US	Mar. 22, 1928	Masonry	--	56.4	4.7·10 ⁷	2.0·10 ⁴	1.3·10 ⁰	Costa, 1988
Oros	Brazil	Mar. 26, 1960	Earthen	35.4	35.4	6.5·10 ⁸	1.4·10 ⁴	2.7·10 ¹	Costa, 1988; MacDonald and Langridge-Monopolis 1984;
Hell Hole	Calif., US	Dec. 23, 1964	Earthen	67	35.1	3.1·10 ⁷	7.4·10 ³	2.3·10 ⁰	Costa, 1988; MacDonald and Langridge-Monopolis 1984;
Lawn Lake	Colo., US	July 15, 1982	Earthen	--	7.9	8.4·10 ⁵	5.1·10 ²	9.2·10 ¹	Jarrett and Costa, 1986
Porter Hill	Oregon, US	Feb. 27, 1993	Earthen	2.5	2.5	1.5·10 ⁴	3.1·10 ¹	2.7·10 ¹	Costa and O'Connor, 1995
Meteorologic floods									
Amazon River	Obidos, Brazil	Mar.-Sept. 1953	Rainfall	n.a.	n.a.	4.0·10 ¹²	3.7·10 ⁵	4.3·10 ³	Oltman et al., 1964
Mississippi River	Vicksburg, Miss., US	March-July, 1973	Rainfall	n.a.	n.a.	4.9·10 ¹¹	5.6·10 ⁴	3.4·10 ³	USGS NWIS (http://water.usgs.gov/nwis)
Columbia River	The Dalles, Oreg., US	May-July, 1894	Rain/Snowmelt	n.a.	n.a.	1.3·10 ¹¹	3.5·10 ⁰⁴	1.4·10 ³	U.S. Army Corp of Engineers, 1958, plate 13
Willamette River	Portland, Oreg., US	Dec. 1964	Rain/Snowmelt	n.a.	n.a.	8.6·10 ⁹	1.3·10 ⁴	3.4·10 ²	Waananen et al., 1970
Plum Creek	Colo., US	June 15, 1965	Rainfall	n.a.	n.a.	3.9·10 ⁷	4.4·10 ³	1.0·10 ¹	Osterkamp and Costa, 1987
Rapid Creek	S.Dak., US	June 9, 1972	Rainfall	n.a.	n.a.	2.5·10 ⁷	1.4·10 ³	1.0·10 ¹	Larimer. 1973
Big Thompson R.	Colo., US	July 31, 1976	Rainfall	n.a.	n.a.	4.7·10 ⁶	8.8·10 ²	3.0·10 ⁰	McCain et al., 1979
McKenzie Creek	Oregon, US	Feb. 6, 1996	Rain/Snowmelt	n.a.	n.a.	1.3·10 ⁸	8.7·10 ²	6.6·10 ¹	G.E. Grant, unpublished data
Lookout Creek	Oregon, US	Feb. 6, 1996	Rain/Snowmelt	n.a.	n.a.	1.9·10 ⁷	1.9·10 ²	6.6·10 ¹	G.E. Grant, unpublished data
H.J. Andrews Exp. Forest (W1)	Oregon, US	Feb. 6, 1996	Rainfall/Snowmelt	n.a.	n.a.	2.9·10 ⁵	2.4·10 ⁰	6.7·10 ¹	G.E. Grant, unpublished data

^aDurations for natural and constructed dam failures calculated from reported values of discharge and volume by assuming a triangular hydrograph. Durations for meteorological floods estimated from published hydrographs or discharge records.

apparent *a priori* reasons why maximum rainfall intensities over timescales ranging from 1 minute to years and delivered by a wide assortment of atmospheric processes should scale so closely with measurement interval, the explanation must lie with the water-holding capacity of the atmosphere, which constrains the amount of rainfall that can occur in time.

These record precipitation values are point measurements. Meteorological floods, however, develop from rainfall over finite areas for which these point measurements are not necessarily representative. While the duration of local maximum precipitation follows a simple scaling relation with measurement interval, depth/area/duration relations, which define the total volume of water delivered to a drainage basin, do not scale so simply (Figure 2b). For all storm durations greater than about 6 hours in the United States, maximum precipitation amounts diminish rapidly for areas greater than about 2,000 km², resulting in total precipitation inputs that are less on a unit area basis for larger basins. This result, which may reflect the maximum size of convection cells within large storms in the U.S. (Figure 1), closely corresponds with patterns of peak discharge per unit area for large floods in the U.S., as will be discussed in following sections.

From these relations (Figure 2), it is apparent that maximum precipitation rate decreases with both duration and the area over which it is measured. But because areally averaged maximum precipitation rates diminish much faster with increasing duration (by about $D^{-0.5}$; Figure 2a) than with increasing area (by $A^{-0.13}$ for storm durations less than 6 hours, and $A^{-0.05}$ for longer duration storms, where A is basin or storm area; Figure 2b), it is smaller basins with faster times of concentration (proportional to $A^{1/2}$) that generate by far the largest discharges per unit area.

Because of seasonal cycles that exist almost everywhere on Earth, a single year is probably the longest timeframe to consider maximum precipitation values with respect to individual flood events. Notable large floods from enhanced precipitation at such long timescales primarily affect very large basins, such as the 1953 flood on the Amazon River (Table 3). Climatic patterns with durations greater than a year, such as ENSO, PDO, and ice ages, are more likely to affect the frequency of flooding rather than being directly responsible for individual flood volumes and magnitudes [e.g. Knox, 1993; Ely *et al.*, 1993], although systems subject to groundwater flooding may be primarily affected by longer duration climatic patterns [e.g. Jones *et al.*, 2000].

The translation of precipitation volumes to flood volumes involves consideration of many other factors that will be described in more detail in following sections. Most of these, such as evapotranspiration during and after precipitation, and losses to snowpack, canopy vegetation,

subsurface, and groundwater storage, reduce the volume of flooding. Additionally, the structure of the surface and subsurface drainage network, which in turn relates to basin geomorphology and geology, controls the delivery of water to channels. Especially for large basins, these factors have substantial influence on flood peak discharges and volumes.

Terrestrial reservoirs

Most floods in human experience are meteorological in origin and derived from atmospheric sources. Indeed, meteorological floods motivate most flood hazard assessment. But the largest floods in Earth history, at least in terms of peak discharge, resulted from rapid release from terrestrial water storage. There are two primary classes of terrestrial storage that can produce large floods: (1) frozen water in glaciers and snowpacks; and (2) waterbodies impounded by natural or constructed dams.

Ice and snow. Although most of the fresh water on Earth is stored within icecaps and glaciers (Table 1), little of this water is available for runoff under the current climate regime. Of the approximately $1.5 \cdot 10^7$ km² of the Earth's surface that is covered by ice, over 86% is in the South Polar regions, with an additional 12% in the North Polar regions [van der Leeden *et al.*, 1990]. The water within these polar ice bodies is in long-term storage with little opportunity to generate runoff in such concentrations as to produce large floods. Much of the remaining 2% of the Earth's surface covered by ice consists of high-elevation glaciers in mid-latitude orogenic belts, and the water within these glaciers is mostly unavailable for flood generation. On timescales relevant for flood generation, rapid melting of ice from glaciers or icecaps probably occurs only during volcanic eruptions, such as Icelandic jökulhlaups and the 1985 eruption of Nevada del Ruiz and consequent lahars in Columbia.

Seasonal snowpacks also store water, with total water storage varying throughout the snow accumulation and melt cycle. Depending on time and location, annual snow water storage can range up to $4 \cdot 10^6$ m³/km², based on maximum-recorded snowfall values [van der Leeden *et al.*, 1990]. Average maximum monthly values for mid-latitude mountain ranges in the U.S. are on the order of $1.7 \cdot 10^6$ m³/km² for the northern Cascade Range, $0.4 \cdot 10^6$ m³/km² for the central Sierra Nevada, and $0.5 \cdot 10^6$ m³/km² for the Rocky Mountains in Colorado, based on SNOTEL data (available at <http://www.wrcc.dri.edu/snotel/snoareas.html>; May 25, 2001). Although volumes of water of this magnitude are potentially available for conversion to streamflow, melt-season release of water from snowpack storage due to sensible heat transfer is generally slower than maximum precipitation rates. Therefore, snow accumulation generally

acts to reduce local peak discharges. For example, melt rates for the 1999 snowpack on Mt. Rainier averaged 8 mm/day, which, if converted directly into runoff, would produce $8 \cdot 10^3 \text{ m}^3/\text{km}^2/\text{day}$ —a value several orders of magnitude lower than rainfall volumes produced by typical storm precipitation intensities (Table 2). Snowmelt floods are generally only notable in very large basins, such as the 1884 flood on the Columbia River (Table 3), where the integrated effects of regional melting can produce larger volumes of water for durations and areas longer and larger than most flood-producing storms.

Snowmelt can substantially contribute to flood flows in basins of all sizes when there is significant snowmelt in conjunction with storm runoff. During rain-on-snow events, rapid melting of snowpacks and release of stored snow water results from both latent and sensible heat fluxes from condensation and warm rain, respectively. In severe rain-on-snow events, such as the December and January 1964–1965 floods in the western United States and the February 1996 floods in the Pacific Northwest, snowmelt may augment total precipitation by 20 to 30% [Risley *et al.*, 1997]. Such events are the dominant flood-producing mechanism for most medium-to-large basins in the Cascade Range of Oregon and Washington. Predicting the magnitude of rain-on-snow events is much more complex than typical watershed routing to predict storm runoff because the amount of local snowmelt and runoff depends on a variety of factors, including elevation, temperature, local wind conditions, snowpack thickness and moisture content, all of which vary tremendously over short distances in the mountainous settings for which rain-on-snow floods are most common. During the February 1996 flood in the Pacific Northwest, some areas of snowpack actually accumulated moisture, thus reducing total storm runoff (unpublished data for the 1996 flood at the H.J. Andrews Long Term Experimental Research Site, Oregon, available at <http://sequoia.fsl.orst.edu/lter/pubs/spclrprfr.html>)

Lakes and Reservoirs. Because floods result from rapid release of large volumes of stored water, lakes and reservoirs are sources of terrestrial water commonly involved in large floods. Such impounded water bodies are an effective cause of large floods because they (1) commonly store large volumes and (2) release water instantaneously to the stream network. Unlike floods generated from atmospheric moisture, floods from rapidly evacuated terrestrial waterbodies can immediately affect a channel without the attenuation due to the time and space scales associated with precipitation rates and integrating flow through a drainage network.

Terrestrial waterbodies commonly involved in floods include ice-, moraine-, and landslide-dammed lakes,

tectonic basins, caldera lakes, and artificial reservoirs impounded by constructed dams. Volumes of stored water in modern terrestrial waterbodies range up to $2.3 \cdot 10^{13} \text{ m}^3$ contained in Lake Baikal, Russia—some three orders of magnitude larger than the volume of water contained in a typical hurricane (Table 2). Nevertheless, the volumes of water involved in floods from historic releases from terrestrial waterbodies are much smaller, the largest being $5.4 \cdot 10^9 \text{ m}^3$ released from a 1986 breach of an ice-dammed lake at Russell Fjord, Alaska (Table 3; Mayo, 1989). This release is approximately equivalent to the volume of water precipitated by large mesoscale convective systems, but smaller than the largest tropical cyclones (Table 2). The largest dam-break floods in the geological record, however, such as the Pleistocene Missoula and Bonneville Floods, had volumes of 10^{12} to 10^{13} m^3 , eclipsing flood volumes generated by historic lake releases and individual storms by two orders of magnitude, but perhaps equivalent in terms of total volume to the largest meteorological floods in large basins from persistent periods of enhanced rainfall (Table 3).

For dam-break floods, breach shape (especially depth) and erosion rate are primary factors controlling peak discharge at the point of failure. Unlike meteorological floods, which develop from spatially distributed inputs that are concentrated through a drainage network, geologic and geomorphic factors do not affect the translation of stored water volumes to the channel during dam breaks, aside from their influence on the nature of the impoundment. For impounded waterbodies that are relatively large with respect to the breach depth (h), peak discharge is proportional to $h^{2.5}$ (also assuming that breach width scales with breach depth) because of the limiting condition of critical flow through the breach [Walder and O'Connor, 1997]. Peak discharge is less strongly correlated with impounded volume because incomplete failure may result in only partial evacuation of storage reservoirs [Webby and Jennings, 1994], and because of the imperfect correlation between breach height and storage volume [Walder and O'Connor, 1997].

To summarize, floods are generated from both atmospheric and terrestrial sources of water, both of which can be defined by both their storage volumes and timescales of release. Individual storms can produce up to $2 \cdot 10^{11} \text{ m}^3$ of water over areas of $1 \cdot 10^6 \text{ km}^2$ for periods of up to several days and are the primary cause of meteorological floods in small basins. Climate and weather patterns that persist for weeks to years generate even larger volumes over larger areas and are the primary cause of large meteorological floods in large basins, with total flood volumes as great as 10^{10} to 10^{12} m^3 . The most important terrestrial source of water for floods is impounded waterbodies. Floods from breached impoundments directly enter the channel, and thus

Table 4. Quaternary floods with discharges greater than 100,000 m³/s.

Flood/River	Location	Date ^a	Peak Discharge (10 ⁶ m ³ /s)	Mechanism	Reference
Kuray	Altai, Russia	Late Pleistocene	18	Ice-dam failure	Baker et al., 1993
Missoula	Northwestern USA	Late Pleistocene	17	Ice-dam failure	O'Connor and Baker, 1992
Darkhat Lakes	Mongolia	Late Pleistocene	4	Ice-dam failure	Grosswald, 1987 (in Rudoy, 1998)
Jassater Lakes	Altai, Russia	Late Pleistocene	2	Ice-dam failure	Grosswald, 1987 (in Rudoy, 1998)
Yaloman lakes	Altai, Russia	Late Pleistocene	2	Ice-dam failure	Grosswald, 1987 (in Rudoy, 1998)
Ulymon Lakes	Altai, Russia	Late Pleistocene	1.9	Ice-dam failure	Grosswald, 1987 (in Rudoy, 1998)
Katla	Iceland	AD1918	1.5	Sub-glac. vol. eruption	Jonsson, 1982
Lake Agassiz	Alberta, Canada	9900 yr BP	1.2	Proglacial-lake overflow	Smith and Fisher, 1993
Aniakchak	Alaska, USA	Late Holocene	1.0	Caldera-lake breach	Waythomas et al., 1996
Lake Bonneville	Northwestern USA	Late Pleistocene	1.0	Lake-basin overflow	O'Connor, 1993
Lake Regina	Canada/USA	Late Pleistocene	0.8	Ice-dam failure	Lord and Kehew, 1987
Jökulsá á Fjöllum	Iceland	Early Holocene	0.7	Sub-glac. vol. eruption	Waite, in press
Indus River	Pakistan	AD1841	0.54	Landslide-dam failure	Shroder et al., 1991
Amazon River	Obidos, Brazil	AD 1953	0.37	Rainfall	Rodier and Roche, 1984
Wabash River	Indiana, USA	Late Pleistocene	0.27	Ice-dam failure	Vaughn and Ash, 1983
Toutle River	Northwestern USA	2,500 yr BP	0.26	Landslide-dam failure	Scott, 1989
Amazon River	Obidos, Brazil	AD 1963	0.25	Rainfall	Rodier and Roche, 1984
Amazon River	Obidos, Brazil	AD 1976	0.24	Rainfall	Rodier and Roche, 1984
Columbia River	Northwestern USA	500 yr BP	0.22	Landslide-dam failure	O'Connor et al., 1996
Lake Agassiz	Canada/USA	9500 yr BP	0.20	Proglacial-lake overflow	Teller and Thorliefson, 1987
Lena River	Kasur, Russia	AD 1967	0.19	Ice-jam and snowmelt	Rodier and Roche, 1984
Lena River	Kasur, Russia	AD 1962	0.17	Ice-jam and snowmelt	Rodier and Roche, 1984
Lena River	Kasur, Russia	AD 1948	0.17	Ice-jam and snowmelt	Rodier and Roche, 1984
Lake Agassiz	Northcentral USA	Late Pleistocene	0.13	Ice-dam failure	Matsch, 1983
Porcupine River	Alaska, USA	Late Pleistocene	0.13	Ice-dam failure	Thorson, 1989
Russell Fjord	Alaska, USA	AD 1986	0.11	Ice-dam failure	Mayo, 1989
Yangtze River	China	AD 1870	0.11	Rainfall	Rodier and Roche, 1984

^aDates reported as "yrs BP" are on basis of radiocarbon dating and have not been calibrated to calendar years.

are capable of producing tremendous peak discharges. Maximum volumes from historic breached impoundments are about 10⁹ m³, but Pleistocene ice-dam failures released volumes of 10¹²-10¹³ m³—volumes similar to the largest meteorological floods.

THE WORLD'S LARGEST FLOODS.

Specific consideration of the Earth's largest known floods provides perspective on the causes of the most extreme floods and patterns of their geographic and geologic settings. We use two complementary data compilations: (1) geologic and historic records of the world's largest known Quaternary floods, of cause and (2) the largest gaged meteorological floods from the world's largest basins. The first compilation emphasizes natural dam

failures and provides insights on the great diversity and scales of flood-generating mechanisms and their particular settings in space and time. The second provides a basis for discussing the geologic, climatologic, and physiographic settings of large meteorological floods from large basins on a global basis. This latter discussion in turn leads to the next section, where we describe the distribution of relatively large meteorological floods from basins of all sizes in the U.S.

The Largest Floods in the Quaternary

We have compiled from various sources a listing of 27 freshwater floods known to have had peak discharges greater than 1·10⁵ m³/s during Quaternary time (Table 4, Figure 3, also on CD). Undoubtedly, there have been many more for which there are no systematic or paleohydrologic

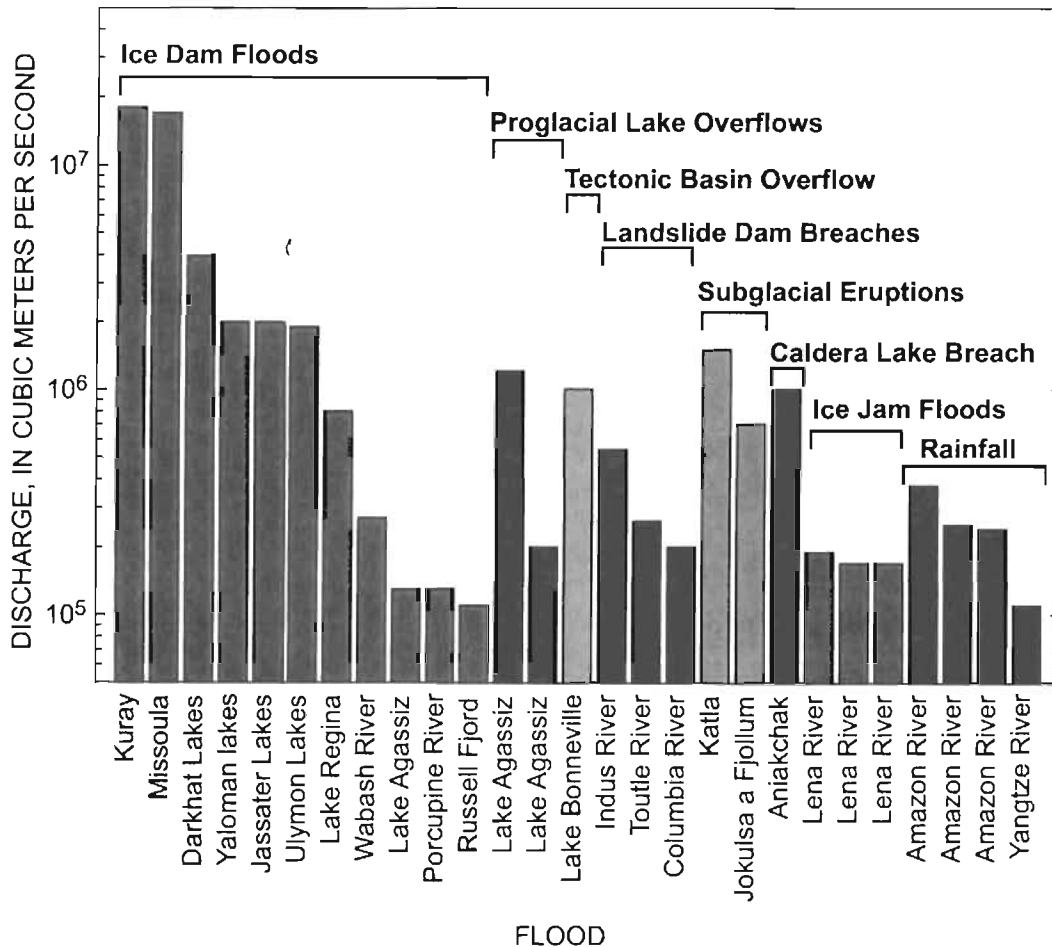


Figure 3. Quaternary floods with discharges greater than 100,000 m³/s, arranged by causative process. From data of table 4.

measurements. Nevertheless, we can draw some fundamental inferences from this partial list as well as from other documented large floods and paleofloods.

All known terrestrial floods with discharges greater than $5 \cdot 10^5$ m³/s resulted from rapid release of water stored behind natural dams or within glaciers (Table 4, Figure 3). The largest known floods of the Quaternary had peak discharges of about $2 \cdot 10^7$ m³/s and resulted from breaches of glacial-age ice dams that blocked large mid-continent drainage systems. Most of the other largest floods ever documented resulted from breaches of natural dams, including landslide dams, ice dams, releases from caldera lakes, and ice-jam floods. Only 4 of the 27 largest documented floods were primarily the result of meteorological conditions and atmospheric water sources. However, if only historic events are considered, the proportion of large meteorological floods rises to 4 of 10.

Floods from Ice-Dammed Lakes

The largest floods in Earth history have resulted from derangement of drainage networks. During the Quaternary, interactions of continental ice sheets with marginal drainage systems have been a primary source of landscape-shaping floods. These floods include the $2 \cdot 10^7$ m³/s Missoula Floods along the Cordilleran Ice Sheet margin [e.g. Bretz, 1923, 1969; Baker, 1973; O'Connor and Baker, 1992], giant floods along the margins of the Laurentide Ice Sheet [e.g. Kehew and Lord, 1987; Lord and Kehew, 1987; Thorson, 1989; Teller and Kehew, 1994], and more recently discovered giant Pleistocene floods in central Asia [e.g. Baker et al., 1993; Rudoy and Baker, 1993, Rudoy, 1998]. These floods all resulted from rapid release of water impounded either in (1) preexisting river valleys dammed by ice or (2) proglacial lakes formed along isostatically

depressed glacial margins. Similar but much smaller floods have occurred historically [Walder and Costa, 1996], including the 1986 flood of 105,000 m³/s resulting from the failure of the dam formed by Hubbard Glacier across Russell Fjord (Table 4; Mayo, 1988).

The large ice-sheet margin floods occurred during glacial ages when, ice sheets had advanced across preexisting drainage networks. Known cases are primarily from the northern mid-latitudes where the present geometry of landmasses supported large continental ice sheets that advanced southward and disrupted large drainage systems. The largest floods (in terms of peak discharge) have been in areas of significant relief at icesheet margins, causing deep valleys to be filled by relatively tall ice dams that impounded very large lakes. When tall dams cataclysmically fail, such as the circa 600-1000 m high dams for the Kuray and Missoula Floods in Asia and North America (Tables 3 and 4), very large peak discharges result because of the exponential dependence of discharge to breach depth [Walder and Costa, 1996].

Basin Breach Floods

Filling and spilling of tectonic basins can also cause large floods. A common scenario is when a hydrologically closed tectonic basin fills with water, resulting in erosion of the basin divide and release of a large volume of water into adjacent drainages. Such was the case for the Bonneville Flood of North America [Gilbert, 1890; Malde, 1968; O'Connor, 1993], which resulted from Pleistocene Lake Bonneville filling the Bonneville Basin, overtopping and eroding alluvial fan sediment that formed the drainage divide at Red Rock Pass, Idaho, and then spilling northward into the Snake River basin. Nearly $5.0 \cdot 10^{12}$ m³ of water was released at a peak discharge of about $1.0 \cdot 10^6$ m³/s during incision of about 100 m of the alluvial barrier. There have likely been similar floods from the many other closed basins in the North American Basin-and-Range province, where there is evidence of incision of surface overflow channels at basin rims [e.g. Currey, 1990] or where there are downstream bouldery deposits [e.g. Anderson, 1998].

Geologic and archeologic records also document tremendous marine floods into tectonically closed basins. The largest known example is the flooding of the Mediterranean basin through a breach developed at the Straits of Gibraltar [Hsu, 1983]—an event now recognized to have caused the faunal upheaval used by Charles Lyell to divide the Miocene and Pliocene epochs [Hsu, 1972]. More recently, Ryan and Pitman [1999] proposed flooding of the Black Sea basin about 7,500 years ago by water from the rising Mediterranean Sea when it overtopped and eroded a divide at the present-day Bosphorus Strait. Ryan and Pitman

[1999] further speculated that this event was the biblical Noah's Flood.

A common element of these floods from and into hydrographically closed basins is that they all occurred in semi-arid environments during times of changing hydrologic conditions. Very large terrestrial freshwater floods are generally associated with sustained periods of positive water balances accompanying changing climatic conditions. Likewise, marine floods are most likely during times of rising sea level due to warming and deglaciation. Large closed basins are preferentially located in tectonically active regions within the arid subtropical belts. In these regions, long periods of negative water balances allow basin development to proceed without continuous overflow and incision of the flanking topographic divides, thus creating the potential for large water volumes to descend over steep sills during rare times of basin filling. Likewise, episodes of marine floods into closed basins are mainly from semi-arid areas where high evaporation rates kept water levels well below sea level, thus providing the hydraulic head necessary for cataclysmic marine water inflow.

Floods Related to Volcanism

Volcanism has been directly or indirectly responsible for 5 of the 27 largest global floods (Figure 3). Some of the largest volcanic floods resulted from eruptions melting substantial snow and ice, including the largest known historic flood of $1.5 \cdot 10^6$ m³/s that accompanied a subglacial volcanic eruption at Katla, Iceland, in 1918 (Table 4; Jonsson, 1982). Similarly, a $0.7\text{--}1.0 \cdot 10^6$ m³/s flood down Jökulsá á Fjöllum, Iceland, was caused by a subglacial eruption about 7,000 years ago [Waiitt, in press].

Volcanic eruptions have also caused floods by means other than direct melting. Debris dams formed during volcanic eruptions by lava flows, lahars, pyroclastic flows, and landslides have blocked drainages, allowing lakes to form and breach. A flow of about $2.6 \cdot 10^5$ m³/s coursed down the Toutle River, Washington, about 2,500 years ago when a landslide associated with an eruption of Mount St. Helens blocked a river valley, and the resulting ancestral Spirit Lake breached cataclysmically [Scott, 1989]. Similar floods would have been likely after the 1980 Mount St. Helens eruptions if mitigation measures had not been undertaken [Sager and Chambers, 1986]. Large floods resulting from breached volcanogenic blockages have also been reported for the circa 700 yr BP eruption of Tarawera Volcano, New Zealand (pers. commun. with Katy Hodgson, Lincoln University, New Zealand, 2000) and for the circa 7,700 yr BP Mt. Mazama eruption in the Oregon Cascades [Conaway, 1999]. Large historic floods in conjunction with volcanism have been reported in southern Mexico, Japan,

and Alaska [Costa, 1988]. There have been at least two large Quaternary floods on the Colorado River in the Grand Canyon, Arizona, from breaches of lava dams [Hamblin, 1994; Fenton *et al.*, this volume].

Floods from breaches of water-filled calderas have also caused large flows, including a late Holocene flood of about $1 \cdot 10^6$ m³/s from Aniakchak Volcano in Alaska [Waythomas *et al.*, 1996], a flood 1800 years ago from Lake Taupo, New Zealand [Marville *et al.*, 1999], and a late Holocene flood from Newberry Caldera in Oregon [Chitwood and Jensen, 2000]. Waythomas *et al.* [1996] suggested that such floods are a common and important geomorphic process in volcanic terrains—an observation corroborated by conditions in the central volcanic zone of New Zealand's North Island, where much of the present drainage system has been formed or affected by large floods from breached caldera lakes (pers. commun. with Vernon Manville and Colin Thorne, Institute of Geological and Nuclear Science, Taupo, New Zealand, 2000).

With the exception of Iceland, which is the only oceanic hot spot or mid-island ridge volcanic center with substantial glacial ice, most documented volcano-related floods are within the Pacific Rim. This could be primarily a function of the detailed hazard analyses that have been done for many of these volcanoes, but it may also reflect the abundant volcanoes in locations of high moisture regimes, especially snow- and ice-covered continental margin volcanoes at temperate latitudes.

Floods From Breached Landslide Dams

Failures of landslide dams not directly related to volcanic activity were the cause of 2 of the 27 largest floods (Table 4). Dam-breach modeling indicates that a flood with a peak discharge of about $5.4 \cdot 10^5$ m³/s resulted from breaching of an 1841 rockslide that temporarily blocked the Indus River within the western Himalayas, Pakistan [Shroder *et al.*, 1991]. Similarly, there is stratigraphic evidence of a flood of about $2.2 \cdot 10^5$ m³/s from breaching of a circa 500 yr BP landslide dam across the Columbia River in western Washington [O'Connor *et al.*, 1996].

Landslide dams can form in a wide range of physiographic settings, from high alpine debris avalanches to quick-clay failures in wide valley floors [Costa and Schuster, 1988]. The most common mechanisms triggering dam-forming landslides are rainstorms, rapid snowmelt, and earthquakes. Landslide dams can be unstable and subject to failure because they have no controlled outlet. The vast majority of dam failures and ensuing floods result from overtopping and incision of the blockage, generally beginning soon after impounded water first reaches the low point of the blockage [Costa and Schuster, 1988].

Despite representing only a small percentage of the world's largest floods, breaches of landslide dams have been

recognized as a significant hazard [e.g. Evans, 1986; Schuster and Costa, 1986; Costa, 1988; Costa and Schuster, 1988, 1991; Clague and Evans, 1994; Walder and O'Connor, 1997; Hewitt, 1998] and have been the focus of several paleoflood studies [e.g. Shroder *et al.*, 1991; O'Connor *et al.*, 1996, O'Connor and Grant, 1999]. There have been at least six historic landslide dam floods with peak discharges greater than $1 \cdot 10^4$ m³/s (see compilation of Walder and O'Connor [1997]). Most of these large floods were associated with tall blockages of large rivers, including cases where breach depths ranged up to 150 m through landslide dams that were as high as 250 m. Similar to the case of glacial dams, the potential peak discharge through a landslide dam scales with the 1.5-to-2.5 power of blockage height [Walder and O'Connor, 1997]. Consequently, landscapes that generate large landslides forming tall blockages in confined valleys have the greatest potential for extreme floods. Larger floods are typically on larger rivers because there are generally larger volumes of water impounded behind dams that form in large river valleys, which in turn results in more erosion and larger breach depths at the dam [Webby and Jennings, 1994].

Landslide dams can dwarf human-constructed dams and therefore produce much larger floods. The largest landslide dam on Earth is the 550 m high Usoy landslide dam in Tajikistan, which formed following a large earthquake in 1911 [Schuster, 2000]. This dam is nearly twice the height of the largest constructed dam in the world today, the 300-m-high Nurek rockfill dam, also in Tajikistan. The largest flood documented from failure of a constructed dam is the Teton Dam, Idaho, which failed in 1976 by piping (Table 3) and for which the peak discharge was about $6.5 \cdot 10^4$ m³/s, less than half the peak discharge of floods resulting from the landslide dam failures listed in Table 4.

Ice-Jam Floods

Three of the world's largest 27 recorded flows were ice-jam floods on the Lena River, (Table 4) Russia—and this does not include the "unprecedented flooding" of May 1998 (<http://www.ncdc.noaa.gov/ol/climate/research/1998/topB99.html>) for which we have been unable to obtain discharge information. Floods on large rivers from ice jams result from "breakup jams" [Hoyt and Langbein, 1955, p. 31-34; Church, 1988] in which dislodged river ice accumulates at constrictions or river bends, forcing ponding upstream and rapid release of water if the ice dams fail rapidly. Such was the case in April 1952 on the Missouri River, North Dakota, where a failing ice dam resulted in discharge rising from about 2,100 m³/s to more than 14,000 m³/s in less than 24 hours [Hoyt and Langbein, 1955, p. 32-33].

Extreme ice-jam floods are most common in high-latitude north-flowing continental river systems like the Lena River and adjacent large river systems of northern

Eurasia and the MacKenzie River of North America. Large poleward-flowing rivers are especially susceptible to large breakup floods because headwater areas may melt before downstream areas, increasing the potential for large blockages.

Large Meteorological Floods

We have found records of four floods that had discharges greater than $1 \cdot 10^5 \text{ m}^3/\text{s}$ and were due primarily to meteorological causes (Table 4)—the floods of 1953, 1963, and 1976 on the Amazon River at Obidos, Brazil, and the 1870 flood of $110,000 \text{ m}^3/\text{s}$ on the Yangtze River, China. The Amazon River, by far the world's largest river with a drainage basin of $7.05 \cdot 10^6 \text{ km}^2$ that encompasses a vast portion of the equatorial South American Cordillera, is also Earth's most favorably sized and positioned basin to generate very large floods. The Yangtze (Chang Jiang) River flood of 1870 was the largest of a historic record that goes back to AD 1153 [Baker and Kochel, 1988].

Inspection of records of the largest floods from the Earth's largest drainage basins (Table 5, Figures 4 and 5, also on CD) shows that, in general, larger basins produce larger floods. But scatter about this relation is at least partly produced by a pronounced geographic pattern of larger unit discharges (defined as peak discharge per unit area) in the tropics, primarily between 10°S and 30°N (Figure 6, also on CD). The largest floods in large basins within the tropics are primarily derived from rainfall within areas affected by tropical cyclones or strong monsoonal airflow (including the Brahmaputra, Ganges, Yangtze, Mekong, and Huangue River basins) or eastward-draining continental basins such as the Amazon and Orinoco River basins that intercept easterly flows of tropical moisture. The distribution of relatively large floods is skewed northward of the equator by the preponderance of land in the northern hemisphere, promoting northward migration of monsoonal moisture flow driven by orographic lifting over large mountain belts such as the Himalayas [Gupta, 1988].

There are several large basins in the tropics that do not have records of relatively large peak discharges on a global basis. These include the Congo, Niger, Chari, and Sao Francisco River basins that drain large areas of low relief or are isolated from zones of major precipitation. Likewise, many of the horse latitude ($20\text{--}40^\circ$) and mid-continental drainage basins outside areas of seasonal tropical moisture influxes do not produce large floods. Examples include the Murray and Darling River basins in Australia, the Nile River and Zambezi Rivers in Africa, and the Colorado and Mississippi Rivers of North America.

Northward of 40°N , snowmelt and ice jams are important contributors to peak discharges from large basins, forming a group of rivers with flood discharges greater than

the apparent latitudinal limits of flood flows derived primarily from rainfall (Figure 6). Exceptional discharges on the Lena, Yenisey, and Yukon Rivers were augmented by ice jams, but relatively large flows on rivers such as the Columbia and Dnieper Rivers indicate the importance of melting snow to peak flows, especially in mid-latitude basins with substantial relief. With the present configuration of continents, there are no southern hemisphere river basins greater than $500,000 \text{ km}^2$ with peak discharges substantially affected by snowmelt.

The distribution of large drainage basins is itself influenced by geologic environment [Potter, 1978]. The vast majority of river basins greater than $500,000 \text{ km}^2$ drain toward passive continental margins, and many have headwaters in active orogenic belts. Examples include the Amazon, Parana, Congo, and Mississippi Rivers—four of the five largest basins in the world. Fewer basins, such as the Colorado and Nile Rivers, drain towards zones of regional extension although many large basins may have originally formed in zones of continental rifting and extension [Potter, 1978]. Of global basins larger than $500,000 \text{ km}^2$, only the Columbia River in western North America drains toward a plate boundary of active convergence.

Relevance to Landscapes and Paleoflood Studies

The incidence of floods caused by different processes changes through time. Most of the largest documented floods in the past 100,000 years resulted from the failures of natural dams. But conditions that caused some of these natural dams, such as the large ice-dam failures at the margins of continental ice sheets, are now absent. Consequently, Earth history contains "flood epochs"—times when climate and topography collude to produce higher-than-typical frequencies of large floods. For floods with discharges on the order of $10^6 \text{ m}^3/\text{s}$, times of advanced continental ice sheets and rapidly changing global water balances are required. In many locations, these outsized floods from previous flood epochs are dominant forces in establishing regional drainage networks and landscape patterns that persist into times of fewer extreme floods [Baker, 1983]. Even during the Holocene, there is evidence of changing flood frequency that can be attributed to subtle climate change [e.g. Ely et al., 1993; Knox, 1993].

Other geologically controlled cataclysmic floods are probably more evenly distributed in time, at least at timescales of 10^2 to 10^5 years, and the future likelihood and magnitude of such events can be more directly guided by analysis of past events. Within active volcanic provinces, the likelihood of large volcanic eruptions and the consequent flood-generation processes probably does not change significantly over hundreds or thousands of years.

Table 5. Largest meteorologic floods from river basins greater than about 500,000 km² (Fig. 4). Data from Rodier and Roche (1984) except as noted. River and station locations shown on Figure 4.

Basin No.	River Basin ^a	Country	Basin Area (10 ³ km ²) ^b	Station	Station Area (10 ³ km ²)	Station Lat. (deg.) ^c	Station Long. (deg.) ^d	Peak Discharge (m ³ /s)	Date	Flood Type
1	Amazon	Brazil	5,854	Obidos	4,640	-1.9	-55.5	370,000	June, 1953	Rainfall
2	Nile	Egypt	3,826	Aswan	1,500	24.1	32.9	13,200	Sept. 25, 1878	Rainfall
3	Congo	Zaire	3,699	Brazzaville B.	3,475	-4.3	15.4	76,900	Dec. 27, 1961	Rainfall
4	Mississippi ^e	USA	3,203	Arkansas City	2,928	33.6	-91.2	70,000	May, 1927	Rainfall
5	Amur	Russia	2,903	Komsomolsk	1,730	50.6	138.1	38,900	Sept. 20, 1959	Rainfall
6	Parana	Argentina	2,661	Corrientes	1,950	-27.5	-58.9	43,070	June 5, 1905	Rainfall
7	Yenisey	Russia	2,582	Yeniseisk	1,400	58.5	92.1	57,400	May 18, 1937	Snowmelt
8	Ob-Irtysh	Russia	2,570	Salekhard	2,430	66.6	66.5	44,800	Aug. 10, 1979	Snowmelt
9	Lena	Russia	2,418	Kasur	2,430	70.7	127.7	189,000	June 8, 1967	Snowmelt/Ice Jam
10	Niger	Niger	2,240	Lokoja	1,080	7.8	6.8	27,140	Feb. 1, 1970	Rainfall
11	Zambezi	Mozambique	1,989	Tete	940	-16.2	33.6	17,000	May 11, 1905	Rainfall
12	Yangtze	China	1,794	Yichang	1,010	30.7	111.2	110,000	July 20, 1870	Rainfall
13	Mackenzie	Canada	1,713	Norman Wells	1,570	65.3	-126.9	30,300	May 25, 1975	Snowmelt
14	Chari	Chad	1,572	N'Djamena	600	12.1	15.0	5,160	Nov. 9, 1961	Rainfall
15	Volga	Russia	1,463	Volgograd	1,350	48.5	44.7	51,900	May 27, 1926	Snowmelt
16	St. Lawrence	Canada	1,267	La Salle	960	45.4	-73.6	14,870	May 13, 1943	Snowmelt
17	Indus	Pakistan	1,143	Kotri	945	25.3	68.3	33,280	1976	Rain/Snowmelt
18	Syr Darya	Kazakhstan	1,070	Tiumen-Aryk	219	44.1	67.0	2,730	June 30, 1934	Rain/Snowmelt
19	Orinoco	Venezuela	1,039	P. Angostura	836	8.1	-64.4	98,120	Mar. 6, 1905	Rainfall
20	Murray	Australia	1,032	Morgan	1,000	-34.0	139.7	3,940	Sept. 5, 1956	Rainfall
21	Ganges	Bangladesh	976	Hardings Br.	950	23.1	89.0	74,060	Aug. 21, 1973	Rain/Snowmelt
22	Shatt al Arab	Iraq	967	Hit/Euphrates	264	34.0	42.8	7,366	May 13, 1969	Rain/Snowmelt
23	Orange	South Africa	944	Buchberg	343	-29.0	22.2	16,230	1843	Rainfall
24	Huanghe	China	894	Shanxian	688	34.8	111.2	36,000	Jan. 17, 1905	Rainfall
25	Yukon	USA	852	Pilot Station	831	61.9	-162.9	30,300	May 27, 1991	Snowmelt
26	Senegal	Senegal	847	Bakel	218	14.9	-12.5	9,340	Sept. 15, 1906	Rainfall
27	Colorado ^e	USA	808	Yuma	629	32.7	-114.6	7,080	Jan. 22, 1916	Rainfall
28	Rio Grande ^e	USA	805	Roma	431	26.4	-99.0	17,850	1865	Rain/Snowmelt
29	Danube	Romanis	788	Orsova	575	44.7	22.4	15,900	April 17, 1895	Snowmelt
30	Mekong	Vietnam	774	Kratie	646	12.5	106.0	66,700	Sept. 3, 1939	Rainfall
31	Tocantins	Brazil	769	Itupiranga	728	-5.1	-49.4	38,780	April 2, 1974	Rainfall
32	Columbia ^e	USA	724	The Dalles	614	45.6	-121.2	35,100	June 6, 1894	Snowmelt
33	Darling	Australia	650	Menindee	570	-32.4	142.5	2,840	June, 1890	Rainfall
34	Brahmaputra ^f	Bangladesh	650	Bahadurabad	636	25.2	89.7	81,000	Aug. 6, 1974	Rain/Snowmelt
35	Sao Francisco	Brazil	615	Traipu	623	-9.6	-37.0	15,890	April 1, 1960	Rainfall
36	Amu Darya	Kazakhstan	612	Chatly	450	42.3	59.7	6,900	July 27, 1958	Rain/Snowmelt
37	Dnieper	Ukraine	509	Kiev	328	50.5	30.5	23,100	May 2, 1931	Snowmelt

^aBasins larger than 500,000 km² for which we were unable to find reliable data include the Nelson River in North America; the Jubba, Irharhar, Araye, Tafassasset and Qattar Rivers in Africa, and the Kolyma and Tarim Rivers in Asia.

^bBasin areas from Vörösmarty et al. (2000).

^cDecimal degrees; positive indicates east of the Greenwich meridian.

^dDecimal degrees; positive indicates north of the equator.

^eStation and discharge data from U.S. Geological Survey National Water Information System (<http://water.usgs.gov/nwis>).

^fStation area and drainage basin data from Global Runoff Data Centre in the Federal Institute of Hydrology, Germany (<http://www.bafg.de/grdc.htm>)

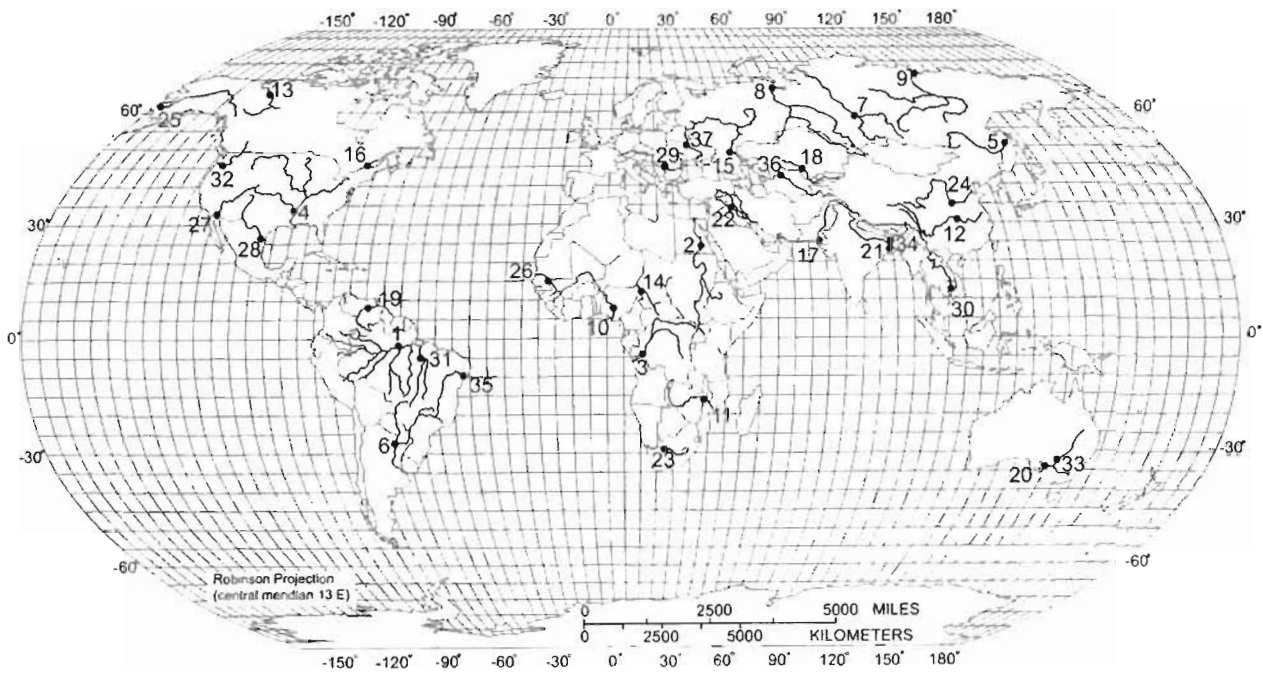


Figure 4. Rivers with drainage areas larger than 500,000 km² listed in Table 5.

Similarly, the frequency of large valley-blocking landslides that accompany large subduction earthquakes probably remains relatively constant over such timescales.

SPATIAL DISTRIBUTION OF THE LARGEST GAGED FLOODS IN THE UNITED STATES.

The types of broadscale relations between physiography and climatology evident in the global distribution of meteorological floods in large basins also appear at continental scales, although the controlling factors involve correspondingly finer scales of physiographic and climatologic interactions. Such continental-scale relations can perhaps be most clearly portrayed by the spatial distribution of large floods in the United States, where the U.S. Geological Survey has a stream-gaging and data-archival program that measures and records flows at several thousand locations throughout the country.

U.S. Geological Survey Annual Flood Data

The basic source of data for this analysis was the "peak flow files" maintained as part of the U.S. Geological Survey National Water Information System [Lupkin and DeLapp, 1979]. These peak flow files are separately maintained for each stream-gaging station and include values for the largest instantaneous discharge for each water year (Oct. 1 to Sept. 30). Data are available for current as well as discontinued

streamgaging stations. In June of 2000, there were records for 23,216 stations that together have more than a million annual peak discharge measurements and estimates. All data were originally measured, reported, and analyzed in English units. Consequently, converting to metric units results in some awkward values in this report and accompanying figures.

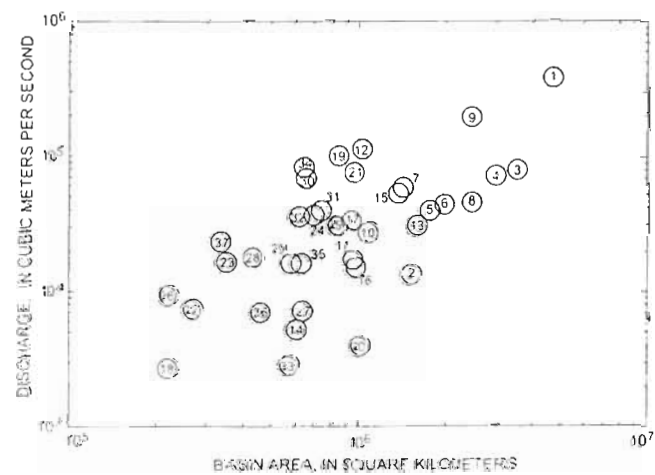


Figure 5. Largest recorded floods from basins larger than 500,000 km² (although many measurements made at locations where only part of the basin contributes) Data keyed to "Basin No." identified in Table 5

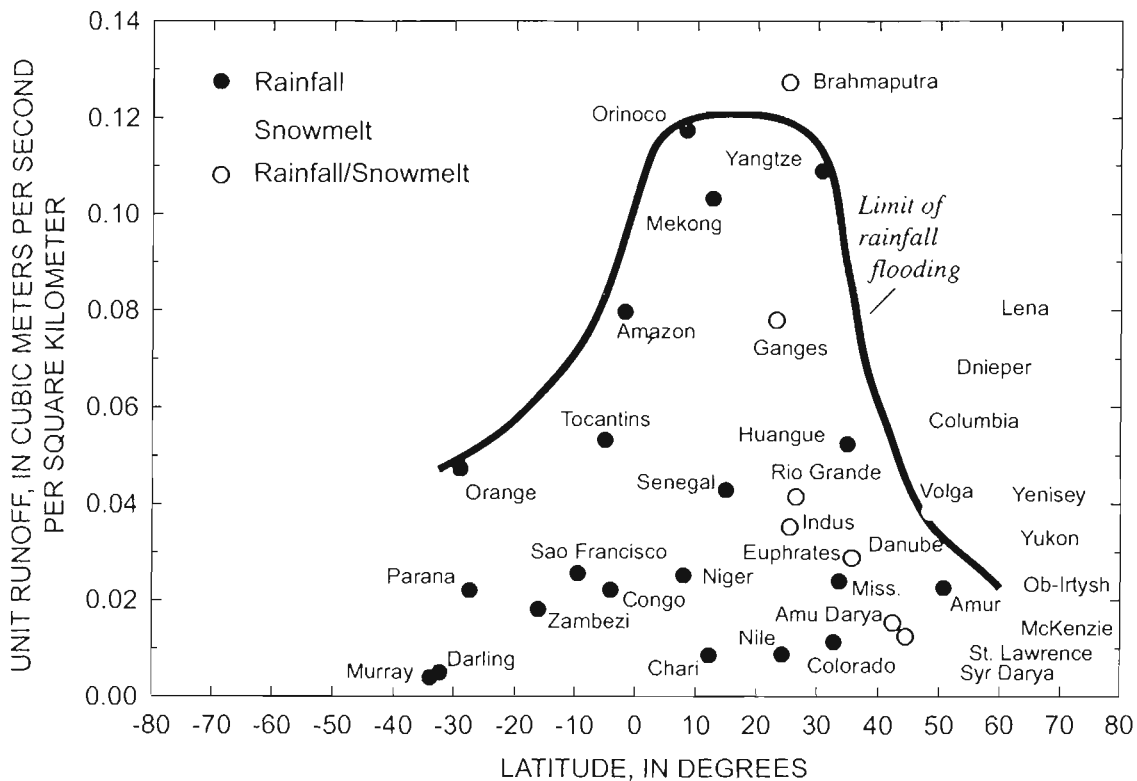


Figure 6. Largest recorded floods from basins larger than 500,000 km² plotted as unit discharge (peak discharge per square kilometer), showing strong latitudinal control on flood size and mechanism. From data of Table 5.

From these peak flow files, we extracted the single largest non-null peak flow (excluding dam failure floods) from all stations with longitude and latitude information and drainage areas greater than 0.26 km² (0.01 mi²), resulting in records of maximum annual peak discharge from each of 22,063 stations (Plate 1, also on CD). Discharge values ranged from 0.03 m³/s to 70,000 m³/s from drainage areas up to the 2.93·10⁶ km² drained by the Mississippi River at Arkansas City, Arkansas (Figure 7, also on CD). These records include estimates for historic peaks at gaging stations dating back to the late 18th century as well as all systematic gaged records through water year 1997 (Sept. 30, 1997). The vast majority of these floods were meteorologic. Some peak discharges have been affected by regulation and diversion, and many are estimates from indirect procedures or from extrapolation of rating curves well beyond measured flows.

To further distinguish the largest of these maximum annual flows at gaging stations relative to drainage area, we selected the flows that exceeded the criteria

$$\begin{aligned} Q &> 15A^{2/3} \text{ for } A < 2,590, \\ \text{and } Q &> 206A^{1/3} \text{ for } A \geq 2,590, \end{aligned} \quad (2)$$

where Q is the peak discharge in cubic meters per second and A is the drainage area in square kilometers. These criteria were formulated to yield a subset of stations with exceptionally large maximum flows (Figure 7), but with an overall distribution of basin areas similar to that of all the stations (Figure 8, also on CD). The maximum discharge at each station exceeds this large-flow threshold for about 13% of the 22,063 stations. The locations of these stations are plotted on Plate 1b, which forms the basis of our conclusions of the physiographic and climatologic controls on large flows within the United States.

The slope decrease for the criterion for drainage areas greater than 2,590 km² (1000 mi²) is necessary to produce a subset of large-flow stations with a distribution of drainage areas similar to that of all stations, thus ensuring an even selection of large-flow stations relative to the distribution of drainage basin areas of gaged streams. Similar slope decreases in unit area peak discharges for larger drainage basins appear in envelope curves bounding the maximum global and U.S. rainfall-runoff floods [Crippen and Bue, 1977; Costa, 1987], as well as for regional compilations [e.g. Enzel et al., 1993]. This decrease in slope for the large-flow criterion separating the largest

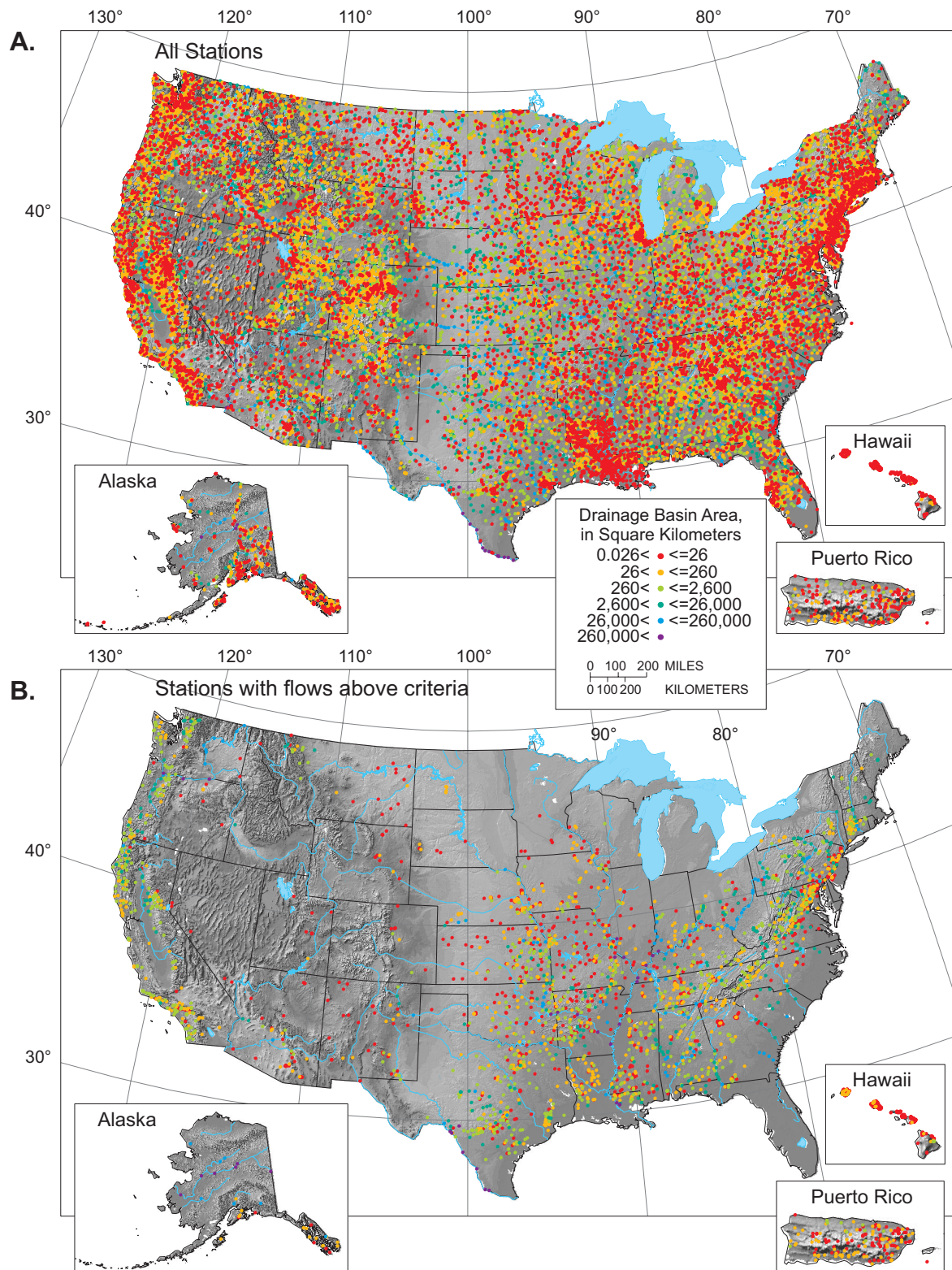


Plate 1. Former and active U.S. Geological Survey stream gages with peak discharge records used in analysis of spatial distribution of large floods, color-coded by basin area. A) All 22,063 former and active sites. B) Large flow sites (2,929) with peak discharges greater than the large-flow criterion described in text.

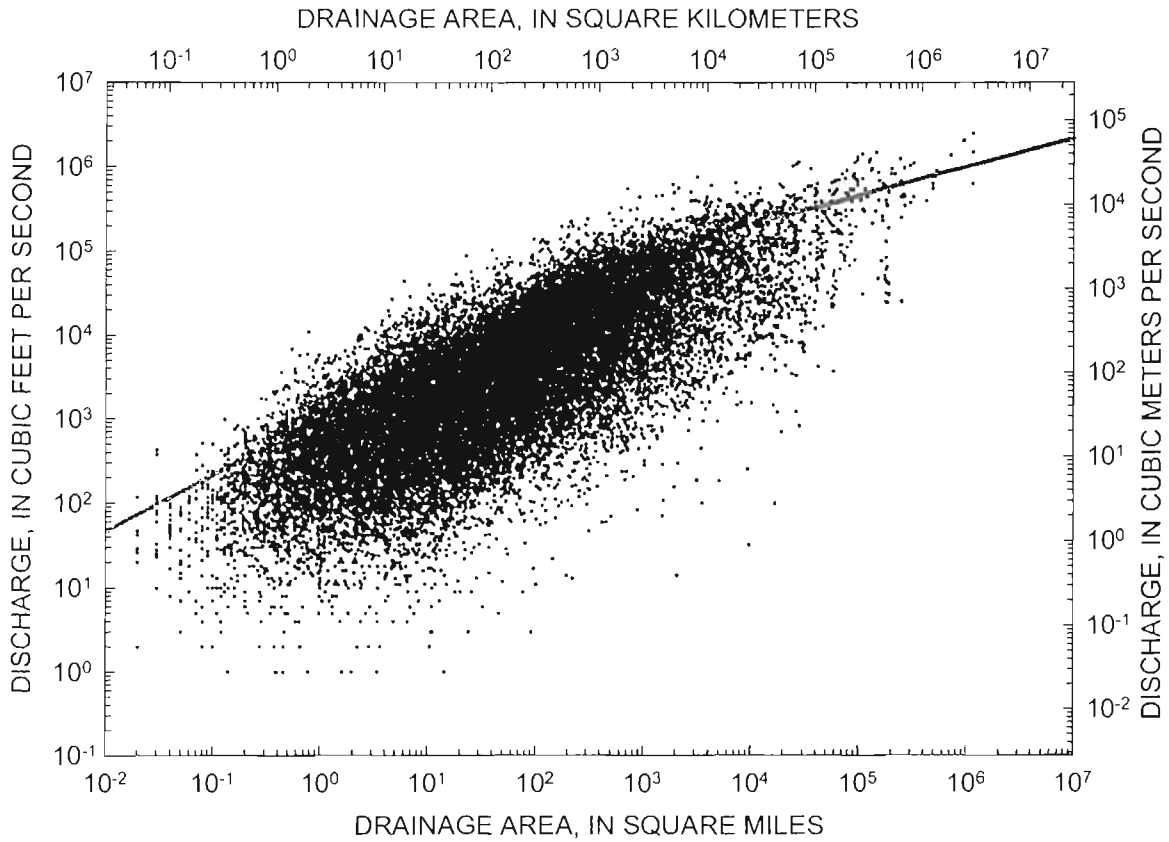


Figure 7. Single maximum flow of record for each of 22,063 former and active U.S. Geological Survey stations with peak discharge records, plotted by station drainage area. Includes records through September 1997

U.S. gaged flows corresponds with the marked decrease in areally averaged rainfall depth for U.S. storms with areas larger than 2,000 km² and durations greater than 6 hours (Figure 2b) and must reflect physical aspects of moisture delivery [Wolman and Costa, 1984], such as limits on storm size and precipitation rates—perhaps corresponding to the spatial extent of intense convective precipitation within tropical storms. Another compounding factor may be that large flows in large basins are probably preferentially attenuated by valley storage [Miller, 1990].

The Spatial Distribution of Relatively Large Flows

The spatial distribution of stations with the largest flow magnitudes relative to drainage area (Plate 1b) is substantially different from the distribution of all stations (Plate 1a), indicating that large flows are concentrated in particular areas. Puerto Rico and Hawaii, where 78% of the 441 stations have maximum station discharges above the delineating threshold, are most subject to relatively large flows. Within the conterminous United States, Plate 1b echos figure 24 of Hoyt and Langbein [1955, p. 75] in which they depicted relative “flood-discharge

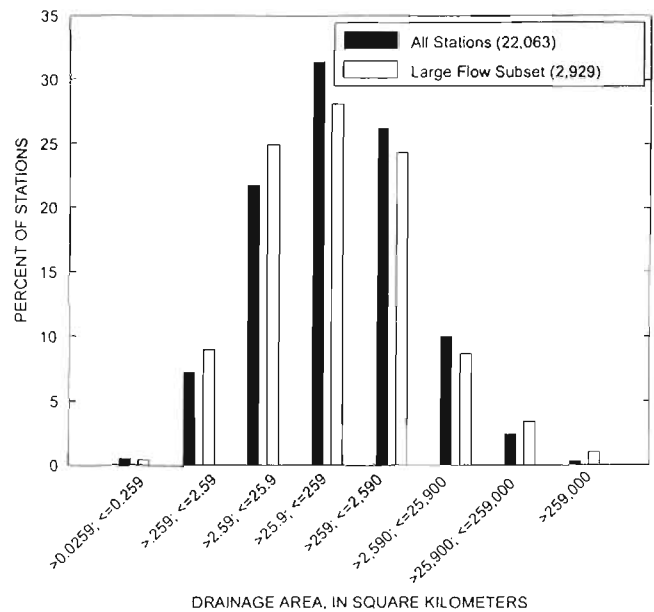


Figure 8. Distribution of all stations and large-flow stations by drainage area.

potentialities." Especially prominent in *Hoyt and Langbein's* map and in Plate 1b are the concentrations of relatively large flows in central Texas and in the central and northern Appalachians. Also indicated on *Hoyt and Langbein's* map and in Plate 1b are relatively high flow magnitudes along the U.S. west coast. One difference that emerges between Plate 1b and *Hoyt and Langbein's* map is in the southeastern Great Plains, an area where the gage network shows many relatively large flows (see also *Michaud et al.* [2001]), but one not noted by *Hoyt and Langbein* for large floods.

There are also broad areas where few measured discharges exceed our large-flow threshold. Only a few stations with small drainage basins in the interior west, especially within the Basin and Range province, have had exceptionally large flows, although this might partly reflect the relative sparseness of stations in this region (Plate 1b). Likewise, the northern tier states of the eastern and midwestern parts of the United States have had few large flows. There have been very few relatively large flows along the Coastal Plain and Florida.

Relations to Regional Climatology and Topography

The overall gradient of decreasing numbers of large floods to the north in general reflects the northward-decreasing gradient of atmospheric water content. But in detail, the flood potential of specific areas is determined by combined roles of geographic setting, regional climatology and topography, which in turn relate to geologic setting. Many of the climatologic and topographic factors controlling flooding in the United States were described in detail by *Hirschboeck* [1991] and are corroborated by the distribution of large floods plotted in Plate 1b.

Within this overall pattern are finer scale relations between regional climatology, topography, and the likelihood of large flows. Puerto Rico and Hawaii both have high frequencies of large floods because they are areas of local orographic lifting in the midst of the tradewind belt, where moisture-laden convective systems and tropical storms are intercepted and convectively lifted by the island mountain ranges. It follows that a greater proportion of stations with the largest flows are on the windward (east) side of these island complexes.

Within the eastern U. S., the pattern of large flows closely corresponds to the gradients of subtropical moisture derived from the Gulf of Mexico and the Atlantic Ocean (compare with figure 23 in *Hirschboeck* [1991]). Finer-scale patterns within this region, however, are clearly linked to topography and geology. Orographic lifting of Gulf of Mexico moisture has caused concentrations of large floods at topographic features such as the Balcones Escarpment in south-central Texas, the Sand Hills of western Louisiana,

the Ozark Mountains of western Missouri, the Flint Hills of eastern Kansas, and along the eastern edge of the Appalachians on the eastern seaboard. *Baker* [1977] described in detail the role of climatic and physiographic controls on flood runoff for streams draining the Balcones Escarpment. The important role of orographic lifting is also illustrated by the lack of exceptional discharges in Florida and along the Coastal Plain of the southern and eastern tier states. Despite being closest to the moisture sources and subject to frequent landings of major hurricanes, these relatively flat areas lack the relief necessary to drive orographic precipitation. Once, however, moisture from hurricanes and their remnants intercepts eastern Appalachia, orographic lifting and efficient runoff concentration can produce exceptional flows [*Miller*, 1990]. The high incidence of relatively large flows in the central and southern midwest and upper Mississippi Valley is partly due to mesoscale convective complexes—large, multiple-celled, and persistent thundercell systems fed largely by moisture from the Gulf of Mexico [*Hayden*, 1988; *Hirschboeck*, 1991]. The Rapid City, South Dakota, flood of 1972 and the Big Thompson River, Colorado, flood of 1976 were caused by such systems. Within the zone of influence of Gulf of Mexico moisture, there are a variety of moisture delivery processes that have caused large flows, including individual thunderstorm cells, mesoscale convective complexes, Atlantic hurricanes, and quasi-stationary upper atmosphere circulation patterns producing several weeks or months of persistent precipitation. These processes are of such diverse temporal and spatial scales that there does not seem to be any systematic pattern of drainage basin size associated with exceptionally large flows (Plate 1b). The only exception is along the Coastal Plain of the southeastern U.S., where only larger rivers draining upland areas have produced large flows, primarily from hurricanes.

West of about longitude 105° west, approximately corresponding to the eastern limit of the Rocky Mountains, moisture from the Pacific Ocean chiefly influences flooding within the conterminous United States and Alaska. Consequently, the stations with largest flows are concentrated along the states contiguous to the Pacific Ocean. The interior western U.S. states of Idaho, Nevada, Utah, Wyoming, and Colorado have very few stations with large flows, and, furthermore, the interior west stations that have had relatively large flows generally represent small basins (less than 26 km²) influenced by isolated thunderstorms. The distribution of stations with the largest flows within the interior West clearly reflects orographic lifting associated with local topographic features such as (1) the eastern limits of the Cordilleran orogenic belt in eastern Wyoming, central Colorado, and eastern New Mexico, (2) the Wasatch Front in Utah, and (3) the Central Highlands and Mogollon Rim in Arizona.

Orographic effects are even more pronounced, however, along the western continental margin of North America. The mountains of southeastern Alaska, the Cascade Range of Oregon and Washington, the Coast Ranges of Washington, Oregon, and California, and the Sierra Nevada and San Gabriel Mountains of California all strongly influence the distribution of stations with large flows. In Oregon, Washington, and Northern California, north-south trending mountain ranges intercept the westerly flow of extratropical cyclones from the Pacific Ocean. The largest floods for most basins are winter floods caused by intense cyclonic storms or the combined effects of cyclonic storms and coincident snowmelt. The extensive winter floods of 1964 and 1996 in the Pacific Northwest were the product of substantial rain-on-snow events. Because these types of events persist for several days, it is the larger basins—generally those with areas of 10^2 to 10^5 km²—that are preferentially affected by these types of events (Plate 1b).

The big basins of the western U.S. that drain extensive areas of the North American Cordillera affected by winter snowfall, such as the Yukon and Columbia Rivers, also produce relatively large flows, invariably in late spring and summer. These large northern basins are the only ones for which snowmelt alone appears to be capable to produce flows greater than our large flow criteria.

Large flows in southern California and Arizona are from mixed sources [Hirschboeck, 1985; 1991], including extratropical cyclonic systems, dissipating tropical storms moving northward from the Pacific, mesoscale convective complexes, and local convective thunderstorms. Consequently, there is substantial variation in the size of basins and seasonality of the largest flows [Hirschboeck, 1985]. The east-west orientation of the Transverse Ranges of southern California and the Mogollon Rim of central Arizona promotes interception of moisture from northward incursions of Pacific tropical storms; consequently, there are distinct concentrations of stations with large floods aligned along these features.

Geologic Controls and Paleohydrologic Implications

Continental position and topography have great influence on the distribution of large floods. In the western United States, the combination of an extensive cordillera associated with a leading continental edge oriented transverse to the mid-latitude belts of westerly cyclonic moisture flow causes relatively large flows to concentrate closely along the continental margin. Similar situations also exist in southern South America and New Zealand [Hayden, 1988]. Smaller areas of uplifted terrain dating to older orogenies, such as the Rocky Mountain Front Range and the

Central Highlands and Mogollon Rim of Arizona also produce small areas of exceptional flows because of their orientation relative to particular tracks of moisture flow. The distribution of large floods in the central and eastern parts of the U.S. corresponds more closely to the broad regional climatology of the overall decreasing moisture gradient away from the Gulf of Mexico. But the specific locations of relatively large floods still clearly relate to distinct topographic features produced by ancient orogenies, such as the Balcones Escarpment, Ozark Mountains, and the margins of the Appalachians.

The spatial distribution of large gaged floods throughout the United States shows that the locations of most of the largest flows can be related to specific combinations of regional climatology and topography. Besides corroborating earlier studies of flood-climate-topography relationships [e.g. Hayden, 1988, and Hirschboeck, 1991], this result leads to more general conclusions about the relation of meteorological floods and geologic environment. In the broadest context, the regional climatology of the conterminous United States is due to the present mid-latitude setting of the continent. At finer regional scales, climatology is influenced by topography, which in turn relates to the geologic history of the continent. Major factors controlling North American topography include the Paleozoic continental collisions that created the Appalachians during amalgamation of supercontinent Pangaea, and subsequent Mesozoic and Cenozoic rifting that allowed weathering and erosion of the Appalachians to form a broad piedmont and coastal plain on the now passive margin of the North American plate. Also during the Mesozoic and Cenozoic, volcanism and deformation along the now active western continental margin have formed the present high-relief topography of the western North American Cordillera. These types of combinations of continental location and geologic history are mirrored on most continents, as well as for past geologic epochs. Thus, understanding the intimate relation between flooding and physiography allows for generalized predictions of regions of relatively large flows elsewhere in the world and back in time.

This perspective can be meaningful for Holocene paleohydrologic research in that it provides context for identifying regions susceptible to exceptionally large flows. Moreover, it shows that regional climate is important in controlling flood magnitude, thus providing rationale for conducting paleoflood studies at sites where millennial scale climate change may be likely to affect flood magnitude and frequency. Further back in time, understanding the relations between climate, continental position and physiography and their effects on flow generation provide grist for understanding paleoenvironments and landscape evolution.

Additionally, paleohydrologic studies can be a useful complement to the gaged records of large floods such as those depicted on Plate 1b. Numerous studies have shown the utility of combining results from paleohydrologic investigations with gaged records to produce better estimates of flood frequency [Kochel *et al.*, 1982; Stedinger and Cohn, 1986; Webb *et al.*, 1988; O'Connor *et al.*, 1994]. Moreover, paleohydrologic methods and studies can perform important checks on gaged records of extreme flows [Enzel *et al.*, 1993; House and Pearthree, 1995], especially for small basins in western North America and other sparsely gaged regions worldwide where critical facilities are commonly designed on the basis of procedures that rely on a few extreme flood measurements.

SUMMARY—LIMITS ON FLOODS.

The preceding sections have described in varying levels of detail the controls on the magnitude of floods from both terrestrial and atmospheric sources as well as the geographic, geologic, and geomorphic environments that foster large floods. At fine scales of space and time, such as the incidence of historic U.S. flooding, important factors are the volumes of water available, and the rate in which it is delivered to the landscape and enters the channel. These factors are dominantly influenced by proximity to moisture sources and local physiography. At broader temporal and spatial scales, such as the global distribution of flooding through the Quaternary epoch, exceptional floods result from particular environmental settings. The Earth's largest floods have resulted from natural-dam failures associated with deranged drainage systems, such as floods resulting from failed ice dams at the margins of continental ice sheets and from filling and spilling of tectonic basins. The largest meteorological floods are primarily associated with the world's largest drainage basins, but are also influenced by topography and position with respect to global patterns of atmospheric circulation. Topography, drainage basin size, and position are the result of geologic processes operating over millions of years and can be linked to particular geologic environments. For example, almost all large basins drain toward passive or extensional continental margins.

Some of these concepts can be further generalized by considering the physical limits of flooding regardless of physiographic or geologic setting. These limits can be formulated and visualized to a first order by considering floods within a Cartesian coordinate space defined by axes of flood volume, peak discharge, and duration (Figure 9, also on CD). These axes are not independent, so such plots cannot be used to derive empirical relations, but they are helpful to show limits to floods posed by physical

properties. A fundamental limit that affects both meteorological and dam-failure floods is continuity: for a triangular hydrograph, continuity requires that,

$$V = 0.5Q \cdot t, \quad (3)$$

where V is flood volume, Q is peak discharge, and t is flood duration, in any consistent set of units. For alternatively shaped hydrographs, the relation is slightly different but of the same order.

For meteorological floods, another fundamental limit arises from interactions between the total volume of water delivered to the basin (a product of the area and precipitation) and the time required to concentrate rainfall distributed across a drainage basin into a channel. This constraint on flood magnitude can be approximately formulated by considering the maximum precipitation rates and volumes summarized previously in conjunction with plausible rates of flow concentration. The maximum discharge at a point of concentration is limited by the product of the contributing area, A , and the precipitation rate measured over some time interval, t :

$$Q_{\max} = A(P/t), \quad (4)$$

where P is precipitation depth. If the maximum velocity of water moving across a drainage basin towards a point of concentration is on the order of 1 m/s, then the contributing area at a given time will be on the order of t^2 ; thus:

$$Q_{\max} = t^2(P/t) = t \cdot P. \quad (5)$$

From figure 2a, the maximum point rainfall data define the empirical relation:

$$P_{\max(\text{point})} = 0.0063t^{0.49}, \quad (6)$$

which is equivalent to (1) but in units of meters and seconds. In the U.S., and perhaps worldwide, however, such point maximum values are applicable for areas on the order of $2.5 \cdot 10^7 \text{ m}^2$, but diminish when measured over large areas [World Meteorological Organization, 1986, p. 103]. For longer-duration storms, areally averaged rainfall decreases by a factor of approximately $A^{-0.05}$ for areas up to $2 \cdot 10^{10} \text{ m}^2$ and by a substantially larger factor for larger areas (Figure 2b). For the purposes here, we will assume that for a given area,

$$P_{\max(\text{areal average})} = 0.0063t^{0.49} (A/(2.5 \cdot 10^7))^{-0.05}, \quad (7)$$

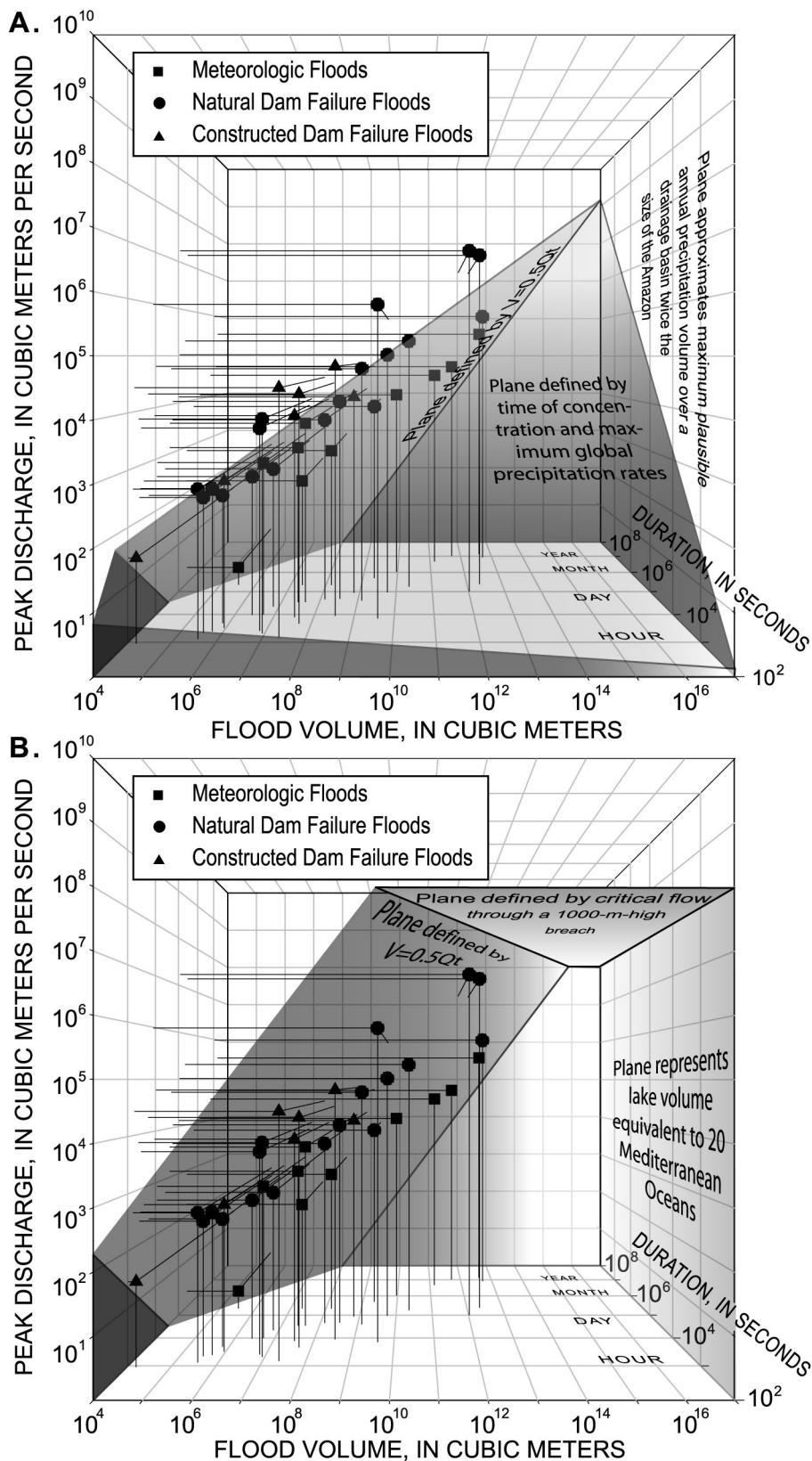


Figure 9. Selected dam-failure and meteorologic floods (from Table 3) in discharge-duration-volume space, showing physical limits to flood magnitude. A) Shaded planes represent physical limits to meteorologic floods, resulting from continuity, time of concentration, and global maximum precipitation rates. All meteorological floods fall within these limits, but many dam-failure floods do not. B) Shaded planes represent physical limits for dam-failure floods, resulting from continuity and critical flow through a maximum plausible terrestrial dam breach. These limits enclose all types of floods.

which reduces to:

$$P_{\max(\text{areal average})} = 0.015t^{0.49}A^{-0.05}. \quad (8)$$

This relation is likely to overestimate maximum plausible precipitation for larger areas, but because the area dependence is small relative to the duration, this approximation is not likely to substantially affect conclusions.

Substituting this relation into (5) yields

$$Q_{\max} = 0.015t^{1.49}A^{-0.05}, \quad (9)$$

which can be expressed in terms of t and V by combining the continuity relation,

$$V = P_{\max(\text{areal average})} \cdot A, \quad (10)$$

and (8), which then results, after algebraic manipulation,

$$Q_{\max} = 0.01t^{1.52}V^{-0.056}. \quad (11)$$

This result may seem somewhat counterintuitive, but recall that both the total flood volume (calculated from maximum global precipitation rates) and the area contributing discharge are highly dependent on the duration.

The plane defined by (11) intersects the plane defined by (3) to enclose a tent-shaped space of meteorological floods with a 'ridgeline' that climbs from low values of flood volume, duration, and peak discharge in the near left corner to large values of volume, duration, and discharge in the far right corner (Figure 9a). Representative data for some exceptional historical meteorological floods (Table 3) plot near this ridgeline for flood volumes ranging between 10^7 to 10^{13} m³.

These relations also allow for speculation on the largest plausible meteorological floods on Earth. For example, a basin twice the size of the Amazon subject to a year's duration of the maximum global annual precipitation (approximately 26.5 m) (without evapotranspiration or loss to long-term groundwater storage) could hypothetically generate a flood of 10^{17} m³ with a peak discharge of 10^9 m³/s (Figure 9a). These values are unrealistic, however, for on a vegetated Earth, evapotranspiration reduces total

annual runoff volume—generally by more than 50% for latitudes less than 60°, and by as much as 80 to 100% for latitudes less than 30° and for closed basins [Baumgartner and Reichel, 1975]. Consequently the volume of floods from several months of persistent precipitation over large drainage basins will be substantially less than the total precipitation volume [Langbein *et al.*, 1949]. But prior to the Devonian establishment of land plants and during times when different land mass configurations hosted exceptionally large and high-relief drainage basins, meteorological floods were likely much larger than at present [Schumm, 1968], perhaps with volumes of 10^{13} to 10^{17} m³ with discharges of 10^6 to 10^9 m³/s.

Flood volumes and peak discharges resulting from dam failures are not limited by precipitation rates or the time required for flow to be concentrated into a channel, but primarily by volume of water stored behind the impoundment and the condition of critical flow through the breach [Walder and O'Connor, 1997]. Volumes of existing natural impoundments range up to the $2.3 \cdot 10^{13}$ of water in Lake Baikal and similarly sized freshwater lakes have been cataclysmically released during the Pleistocene (Table 3). Even larger flood volumes have likely been released in more ancient geologic settings, including the circa 10^{16} m³ of water that spilled into the Mediterranean basin at the end of the Miocene Period. Peak discharge for most breached dams is regulated by the condition of critical flow at the breach. For critical flow through a rectangular cross section,

$$Q = 0.54g^{1/2}B \cdot H^{3/2}, \quad (12)$$

where g is the acceleration of gravity (9.8 m/s²), B is the channel width in meters, and H is the difference in elevation in meters between the impounded water surface (away from the zone of drawdown influence) and the bottom of the outlet channel (after King [1954, p. 8.8-8.11]). Other cross-section shapes yield slightly different coefficients but overall results of the same magnitude.

The largest known natural-dam failures have been the 500 to 900 m breaches of Pleistocene ice dams (Table 3). Thus, a blockage 1,000 m high might be an approximate upper limit for terrestrial impoundments subject to failure. If such a blockage were to fail completely with an outlet channel width five times its depth, the maximum discharge

Figure 9. Selected dam-failure and meteorologic floods (from Table 3) in discharge-duration-volume space, showing physical limits to flood magnitude. A) Shaded planes represent physical limits to meteorologic floods, resulting from continuity, time of concentration, and global maximum precipitation rates. All meteorological floods fall within these limits, but many dam-failure floods do not. B) Shaded planes represent physical limits for dam-failure floods, resulting from continuity and critical flow through a maximum plausible terrestrial dam breach. These limits enclose all types of floods.

would be about 10^8 m³/s, approximately five times greater than the largest documented terrestrial floods (Figure 9b). This limit, combined with the limit forced by continuity [expressed by equation (3)], defines a much larger permissible space (within axes defined by discharge, volume, and duration) for dam-failure floods than exists for meteorological floods (Figure 9b). This result is borne out by the observation that several dam-failure floods plot within this space, but outside the limits of potential meteorological floods.

From empirical and theoretical considerations, both meteorological and dam-failure floods can potentially involve volumes of 10^{15} to 10^{17} m³ of water with discharges of 10^6 to 10^8 m³/s. However, meteorological floods with volumes greater than 10^{13} m³ and discharges greater than 10^6 m³/s probably require landscape conditions much different from those that have existed throughout most of the Phanerozoic. In contrast, floods from dam failures have achieved discharges of 10^6 to 10^8 m³/s during the Quaternary, although the largest of these dam failure floods have been associated with altered hydrologic systems during Pleistocene ice ages.

Paleohydrologic research, aided by the tools of stratigraphy, geochronology, and hydrologic and hydraulic analysis, is uniquely poised to investigate floods that span these ranges of sizes and timescales. Nevertheless, the primary concepts brought forward by this paper—that there are likely to be quantifiable limits to floods, that specific arrangements of physiography and climatology can produce especially large floods from a variety of mechanisms, and that certain geologic conditions can foster more and larger floods than others—is not particularly new. Indeed, subplots embedded within these overarching precepts have motivated most of the paleohydrologic research of the last three decades, including much of the research reported in this volume. The framework established here, however, should serve as a rational basis for defining the context of specific floods or flood environments within the changing constellations of geology, physiography, and climatology that produce large riverine floods over the course of Earth history.

Acknowledgments. Discussions with P.K. House, V.R. Baker, and J.A. Smith aided in development of the ideas presented here. T. Haluska, L. Orzol, and R. Viger assisted with the compilation and analysis of the U.S. Geological Survey flow data. Reviews by E.E. Wohl, P.K. House, A. Gupta, and J. Williams improved the final manuscript.

REFERENCES

- Anderson, D.E., Late Quaternary paleohydrology, lacustrine stratigraphy, fluvial geomorphology and modern hydroclimatology of the Amargosa River / Death Valley hydrologic system, California and Nevada, Ph.D. Dissertation, 521 pp., University of California, Riverside, 1998.
- Baker, V.R., Paleohydrology and sedimentology of Lake Missoula flooding in eastern Washington, *Geol. Soc. Amer. Spec. Pap.* 144, 79 pp., 1973.
- Baker, V.R., Stream-channel response to floods, with examples from central Texas, *Geol. Soc. Amer. Bull.*, 88, 1057-1071, 1977.
- Baker, V.R., Late Pleistocene fluvial systems, in Volume 1, The Late Pleistocene, edited by S.C. Porter, in *Late-Quaternary Environments of the United States*, edited by H.E. Wright, Jr., pp. 115-129, University of Minnesota Press, Minneapolis, Minnesota, 1983.
- Baker, V.R., G. Benito and A.N. Rudoy, Paleohydrology of late Pleistocene superflooding, Altay Mountains, Siberia, *Science*, 259, 348-350, 1993.
- Baker, V.R., and R.C. Kochel, Flood sedimentation in bedrock fluvial systems, in *Flood Geomorphology*, edited by V.R. Baker, R.C. Kochel and P.C. Patton, pp. 123-138, John Wiley and Sons, New York, 1988.
- Barry, R.G. and R.J. Chorley, *Atmosphere, Weather and Climate*, 392 pp., Routledge, New York, 1992.
- Baumgartner, A. and E. Reichel, *The World Water Balance; Mean Annual Global, Continental and Marine Precipitation, Evaporation and Runoff*, 179 pp., Elsevier, New York, 1975.
- Blown, I.G. and M. Church, Catastrophic lake drainage within the Homathko River basin, British Columbia, *Can. Geotech. Jour.*, 22, 551-563, 1985.
- Bretz, J.H., The Channeled Scabland of the Columbia Plateau, *J. Geol.*, 31, 617-649, 1923.
- Bretz, J.H., The Lake Missoula floods and the Channeled Scabland, *J. Geol.*, 77, 505-543, 1969.
- Bradley, A.A. and J.A. Smith, The hydrometeorological environment of extreme rainstorms in the Southern Plains of the United States, *J. Applied Met.*, 33, 14-18, 1994.
- Cayan, D.R. and D.H. Peterson, The influence of North Pacific atmospheric circulation on streamflow in the west, in *Aspects of Climate Variability in the Pacific and the Western Americas*, *Amer. Geophys. Union Mono.* 55, edited by D.H. Peterson, pp. 375-398, 1989.
- Chitwood, L.A. and R.A. Jensen, Large prehistoric flood along Paulina Creek, in *What's New at Newberry Volcano, Oregon*, edited by R.A. Jensen and L.A. Chitwood, pp. 31-40, U.S.D.A. Forest Service, Bend, Oregon, 2000.
- Church, M., Floods in cold climates, in *Flood Geomorphology*, edited by V.R. Baker, R.C. Kochel and P.C. Patton, pp. 205-230, John Wiley and Sons, New York, 1988.
- Clague, J.J. and S.G. Evans, Formation and failure of natural dams in the Canadian Cordillera, *Geol. Surv. Can. Bull.* 464, 35 pp., 1994.
- Conaway, J.S., Hydrogeology and paleohydrology of the Williamson River basin, Klamath County, Oregon, M.S. thesis, 119 pp., Portland State University, Portland, Oregon, 1999.
- Costa, J.E., A comparison of the largest rainfall-runoff floods in the United States with those of the People's Republic of China and the world, *J. Hydrol.*, 96, 101-115, 1987.
- Costa, J.E., Floods from dam failures, in *Flood Geomorphology*.

Anderson, D.E., Late Quaternary paleohydrology, lacustrine stratigraphy, fluvial geomorphology and modern hydroclimatology

- edited by V.R. Baker, R.C. Kochel and P.C. Patton, pp. 439-464, John Wiley and Sons, New York, 1988.
- Costa, J.E. and J.E. O'Connor, Geomorphically effective floods, in *Natural and Anthropogenic Influences in Fluvial Geomorphology*, *Amer. Geophys. Union Mono.* 89, edited by J.E. Costa, A.J. Miller, K.W. Potter and P.R. Wilcock, pp. 45-56, 1995.
- Costa, J.E. and R.L. Schuster, The formation and failure of natural dams, *Geol. Soc. Amer. Bull.*, 100, 1054-1068, 1988.
- Costa, J.E. and R.L. Schuster, Documented historical landslide dams from around the world, *U.S. Geol. Surv. Open-File Rep.* 91-239, 485 pp., 1991.
- Cotton, W.R. and R.A. Anthes, *Storm and Cloud Dynamics*, 883 pp., Academic Press, San Diego, California, 1989.
- Crippen, J.R. and C.D. Bue, Maximum floodflows in the conterminous United States, *U.S. Geol. Surv. Water-Supply Pap.* 1887, 52 pp., 1977.
- Currey, D.R., Quaternary palaeolakes in the evolution of semidesert basins, with special emphasis on Lake Bonneville and the Great Basin, U.S.A., *Palaeogeography, Palaeoclimatology, and Palaeoecology*, 76, 189-214, 1990.
- Dettinger, M. and D. Cayan, The Pacific Decadal Oscillation and flood frequencies in the United States, *Geol. Soc. Amer. Abstr. with Prog.*, 32(7), 460, 2000.
- Ely, L.L., Y. Enzel, V.R. Baker and D.R. Cayan, A 5000-year record of extreme floods and climate change in the southwestern United State, *Science*, 262, 410-412, 1993.
- Enzel, Y., L.L. Ely, P.K. House, V.R. Baker, and R.H. Webb, Paleoflood evidence for a natural upper bound to flood magnitudes in the Colorado River basin, *Water Resour. Res.*, 29, 2287-2297, 1993.
- Evans, S.G., The maximum discharge of outburst floods caused by the breaching of man-made and natural dams, *Can. Geotech. Jour.*, 23, 385-387, 1986.
- Evans, S.G., The breaching of moraine-dammed lakes in the southern Canadian Cordillera, in *Proceedings of the International Symposium on Engineering Geological Environment in Mountainous Areas*, pp. 141-150, Beijing, China, v. 2, 1987.
- Gilbert, G.K., Lake Bonneville, *U.S. Geol. Surv. Mono.* 1, 438 pp., 1890.
- Glazyrin, G.Y. and V.N. Reyzvikh, Computation of the flow hydrograph for the breach of landslide lakes, *Soviet Hydrology*, Selected Papers (published by the American Geophysical Union), Issue no. 5, 492-496, 1968.
- Gupta, A., Large floods as geomorphic events in the humid tropics, in *Flood Geomorphology*, edited by V.R. Baker, R.C. Kochel and P.C. Patton, pp. 301-315, John Wiley and Sons, New York, 1988.
- Hamblin, W.K., Late Cenozoic lava dams in the western Grand Canyon, *Geol. Soc. Amer. Mem.* 183, 139 pp., 1994.
- Hayden, B.P., Flood climates, in *Flood Geomorphology*, edited by V.R. Baker, R.C. Kochel and P.C. Patton, pp. 13-26, John Wiley and Sons, New York, 1988.
- Hewitt, K., Record of natural damming and related floods in the Upper Indus Basin, *Indus*, 10(3), 11-19, 1968.
- Hewitt, K., 1998, Catastrophic landslides and their effects on the Upper Indus streams, Karakoram Himalaya, northern Pakistan, *Geomorphology*, 26, 47-80, 1998.
- Hirschboeck, K.K., Hydroclimatology of flow events in the Gila river basin, central and southern Arizona, Ph.D. Dissertation, 354 pp., University of Arizona, Tucson, Arizona, 1985.
- Hirschboeck, K.K., Flood hydroclimatology, in *Flood Geomorphology*, edited by V.R. Baker, R.C. Kochel and P.C. Patton, pp. 27-49, John Wiley and Sons, New York, 1988.
- Hirschboeck, K.K., Climate and floods, in *National Water Summary 1988-89, Floods and Droughts*, *U.S. Geol. Surv. Water-Supply Paper* 2375, R.W. Paulsen, E.B. Chase, R.S. Roberts and D.W. Moody, compilers., pp. 67-88, 1991.
- Hirschboeck, K.K., Overlapping scales and the atmospheric causes of floods, *Geol. Soc. Amer. Abstr. with Prog.*, 32(7), 460, 2000.
- House, P.K., and P.A. Pearthree, A geomorphologic and hydrologic evaluation of an extraordinary flood discharge estimate: Bronco Creek, Arizona, *Water Resour. Res.*, 31, 3059-3073, 1995.
- Hoyt, W.G. and W.B. Langbein, *Floods*, 469 pp., Princeton University Press, Princeton, New Jersey, 1955.
- Hsü, K.J., Origin of saline giants: a critical review after the discovery of the Mediterranean evaporite, *Earth-Sci. Rev.*, 8, 371-396, 1972.
- Hsü, K.J., *The Mediterranean was a Desert; a Voyage of the Glomar Challenger*, 197 pp., Princeton University Press, Princeton, New Jersey, 1983.
- Jarrett, R.D. and J.E. Costa, Hydrology, geomorphology, and dam-break modeling of the July 15, 1982, Lawn Lake Dam and Cascade Dam failures, Larimer County, Colorado, *U.S. Geol. Surv. Prof. Pap.* 1369, 78 pp., 1986.
- Jarrett, R.D. and H.E. Malde, Paleodischarge of the late Pleistocene Bonneville Flood, Snake River, Idaho, computed from new evidence, *Geol. Soc. Amer. Bull.*, 99, 127-134, 1987.
- Jennings, M.E., V.R. Schneider and P.E. Smith, Computer assessments of potential flood hazards from breaching of two debris dams, Toutle River and Cowlitz River systems, in *U.S. Geol. Surv. Prof. Pap.* 1250, pp. 829-836, 1981.
- Jennings, D.N., M.G. Webby and D.T. Parkin, Tunawaca landslide dam, King Country, New Zealand, *Landslide News*, 7, 25-27, 1993.
- Jones, M.A., J.L. Jones and T.D. Olsen, Ground-water flooding in glacial terrain of southern Puget Sound, Washington, *U.S. Geol. Survey Fact Sheet FS-111-00*, 4 pp., 2000.
- Jonsson, J., Notes on the Katla volcanoglacial debris flows, *Jökull*, 32, 61-68, 1982.
- Kehew, A.E. and M.L. Lord, Glacial-lake outburst along the mid-continent margins of the Laurentide ice-sheet, in *Catastrophic Flooding*, edited by L. Mayer and D. Nash, pp. 95-120, Allen and Unwin, Boston, Massachusetts, 1987.
- King, H.W., *Handbook of Hydraulics (fourth edition)*, uneven pagination, McGraw-Hill, New York, 1954.
- Knox, J.C., Large increases in flood magnitude in response to modest changes in climate, *Nature*, 361, 430-432, 1993.
- Kochel, R.C., and V.R. Baker, Paleoflood hydrology, *Science*, 215, 353-361, 1982.
- Kochel, R.C., V. R. Baker, and P.C. Patton, Paleohydrology of southwestern Texas, *Water Resour. Res.*, 18, 1165-1183, 1982.

- Langbein, W.B. and others (unidentified), Annual runoff in the United States, *U.S. Geol. Surv. Circ.* 52, 14 pp., 1949.
- Larimer, O.J., Flood of June 9-10, 1972, at Rapid City, South Dakota, *U.S. Geol. Surv. Hydro. Inv. Atlas HA-511*, 1 sheet, 1973.
- Leopold, L.B., Areal extent of intense rainfalls, New Mexico and Arizona, *Amer. Geophys. Union Trans.*, 32, 347-357, 1942.
- Lepkin, W.D. and M.M. DeLapp, Peak-flow file retrieval (program 1980), *U.S. Geol. Surv. Open-File Rep.* 79-1336-1, 64 pp. 1979.
- Lliboutry, L., V.M. Arnao, A. Pautre and B. Schneider, Glaciological problems set by the control of dangerous lakes in Cordillera Blanca, Peru: I. Historical failures of morainic dams, their causes and prevention, *J. Glaciology*, 18, 239-254, 1977.
- Lord, M.L., and A.E. Kehew, Sedimentology and paleohydrology of glacial-lake outburst deposits in southeastern Saskatchewan and northwestern North Dakota, *Geol. Soc. Amer. Bull.*, 99, 663-673, 1987.
- Ludlam, F.H., Clouds and storms: *The Behavior and Effect of Water in the Atmosphere*. 405 pp., The Pennsylvania State University Press, Philadelphia, Pennsylvania, 1980.
- MacDonald, T.C. and J. Langridge-Monopolis. Breaching characteristics of dam failures, *J. Hydraul. Eng.*, 110, 567-586, 1984.
- Malde, H.E., The catastrophic late Pleistocene Bonneville Flood in the Snake River Plain, Idaho, *U.S. Geol. Surv. Prof. Pap.* 596, 52 pp., 1968.
- Manville, V., J.D.L. White, B.F. Houghton and C.J.N. Wilson, Paleohydrology and sedimentology of a post-1.8 ka breakout flood from intracaldera Lake Taupo, North Island, New Zealand, *Geol. Soc. Amer. Bull.*, 111, 1435-1447, 1999.
- Matsch, C.L., River Warren, the southern outlet of glacial Lake Agassiz, in *Geol. Assoc. Can. Spec. Pap.* 26, pp. 231-244, 1983.
- Mayo, L.R., Advance of Hubbard Glacier and closure of Russell Fiord, Alaska—Environmental effects and hazards in the Yakutat area, in *U.S. Geol. Surv. Circ.* 1016, pp. 4-16, 1988.
- Mayo, L.R., Advance of Hubbard Glacier and 1986 outburst of Russell Fiord, Alaska, U.S.A., *J. Glaciology*, 13, 189-194, 1989.
- McCain, J.F., L.R. Hoxit, R.A. Maddox, C.F. Chappell and F. Caracena, Storm and flood of July 31-August 1, 1976, in the Big Thompson River and Cache la Poudre River Basins, Larimer and Weld Counties, Colorado: Part A. Meteorology and hydrology in Big Thompson River and Cache la Poudre River Basins, in *U.S. Geol. Surv. Prof. Pap.* 1115, pp. 1-85, 1979.
- Michaud, J.D., K.K. Hirschboeck, and M. Winchell, Regional variations in small-basin floods in the United States, *Water Resour. Res.*, 37, 1405-1416, 2001.
- Müller, A.J., Flood hydrology and geomorphic effectiveness in the central Appalachians, *Earth Surf. Proc. Landf.*, 15, 119-134, 1990.
- Mora, S., C. Madrigal, J. Estrada and R.L. Schuster, The 1992 Rio Toro Landslide Dam, Costa Rica, *Landslide News*, 7, 19-22, 1993.
- More, R.J., Hydrological models and geography, in *Models in Geography*, edited by R.J. Chorley and P. Haggett, pp. 145-185, Methuen, London, 1967.
- O'Connor, J.E. and V.R. Baker, Magnitudes and implications of peak discharges from glacial Lake Missoula, *Geol. Soc. Amer. Bull.*, 104, 267-279, 1992.
- O'Connor, J.E., Hydrology, hydraulics, and geomorphology of the Bonneville Flood, *Geol. Soc. Amer. Spec. Pap.* 274, 83 pp., 1993.
- O'Connor, J.E., L.L. Ely, E.E. Wohl, L.E. Stevens, T.S. Melis, V.S. Kale, and V.R. Baker, A 4,500-year record of large floods on the Colorado River in the Grand Canyon, Arizona, *J. Geol.*, 102, 1-9, 1994.
- O'Connor, J. E., T.C. Pierson, D Turner, B.F. Atwater, and P.T. Pringle, An exceptionally large Columbia River flood between 500 and 600 years ago—Breaching of the Bridge-of-the-Gods Landslide?, *Geol. Soc. Amer. Abstr. Prog.*, 28(7), 1996.
- O'Connor, J.E. and G.E. Grant, Floods, floods, and floods on the Deschutes River, Oregon, in *Proc. of the Second Intern. Paleoflood Conf.*, edited by P.K. House, Prescott, Arizona, p. 35, 1999.
- O'Connor, J.E., J.H. Hardison, III, and J.E. Costa, Debris flows from failures of Neoglacial moraine dams in the Three Sisters and Mt. Jefferson Wilderness areas, Oregon, *U.S. Geol. Surv. Prof. Pap.* 1608, 2001 (in press).
- Oltman, R.E., H.O. Sternberg, F.C. Ames and L.C. Davis, Jr., Amazon River investigations reconnaissance measurements of July 1963, *U.S. Geol. Surv. Circ.* 486, 15 p., 1964.
- Osterkamp, W.R. and J.E. Costa, Changes accompanying an extraordinary flood on a sand-bed stream, in *Catastrophic Flooding*, edited by L. Mayer and D. Nash, pp. 201-224, Allen and Unwin, Boston, Massachusetts, 1987.
- Pena, H. and W. Klohn, Non-meteorological flood disasters in Chile, in *Hydrology of Disasters*, edited by Ö. Starosolszky and O.M. Meldcr, pp. 243-258, James and James, London, 1989.
- Plaza-Nieto, G., Y. Yepes and R.L. Schuster, Landslide dam on the Pisque River, northern Ecuador, *Landslide News*, 4, 2-4, 1990.
- Potter, P.E., Significance and origin of big rivers, *J. Geol.*, 86, 13-33, 1978.
- Risley, J., D. Marks and T. Link, Application of a quasi-energy balance model to simulate snowmelt under variable canopies during a major rain-on-snow event, *EOS, Trans. Am. Geophys. Union (1997 Fall Meeting Supplement)*, 78(46), 320, 1997.
- Rodier, J.A. and M. Roche, World catalogue of maximum observed floods, *Intern. Assoc. Hydrol. Sci. Publ. No.* 143, 354 p., 1984.
- Rudoy, A., Mountain ice-dammed lakes of southern Siberia and their influence on the development and regime of the intracontinental runoff systems of North Asia in the late Pleistocene, in *Palaeohydrology and Environmental Change*, edited by G. Benito, V.R. Baker and K.J. Gregory, pp. 215-234, John Wiley and Sons, Chichester, 1998.
- Rudoy, A.N. and V.R. Baker, Sedimentary effects of cataclysmic Late Pleistocene glacial outburst flooding, Altay Mountains, Siberia, *Sed. Geol.*, 85, 53-62, 1993.
- Ryan, W. and W. Pitman, Noah's flood: *The New Scientific*

- Discoveries about the Event that Changed History*, 319 pp., Simon and Schuster, New York, 1999.
- Sager, J.W. and D.R. Chambers, Design and construction of the Spirit Lake outlet tunnel, Mount St. Helens, Washington, in *Landslide Dams—Processes, Risk, and Mitigation*, Amer. Soc. of Civil Eng. Spec. Publ. No. 3, edited by R.L. Schuster, pp. 42-58, 1986.
- Schumm, S.A., Speculations concerning paleohydrologic controls of terrestrial sedimentation, *Geol. Soc. Amer. Bull.*, 79, 1573-1588, 1968.
- Schuster, R.L., A worldwide perspective on landslide dams, in *Usoi Landslide Dam and Lake Sarez—An Assessment of Hazard and Risk in the Pamir Mountains, Tajikistan, International Strategy for Disaster Reduction Series No. 1*, edited by D. Alford and R. Schuster, pp. 19-22, United Nations, New York, 2000.
- Schuster, R.L. and J.E. Costa, A perspective on landslide dams, in *Landslide Dams—Processes, Risk, and Mitigation*, Amer. Soc. of Civil Eng. Spec. Publ. No. 3, edited by R.L. Schuster, pp. 1-20, 1986.
- Scott, K.M., Magnitude and frequency of lahars and lahar-runout flows in the Toutle-Cowlitz River system, *U.S. Geol. Surv. Prof. Pap. 1447-B*, 33 pp. 1989.
- Shroder, J.F. Jr., K. Cornwell and M.S. Khan, Catastrophic breakout floods in the western Himalaya, Pakistan, *Geol. Soc. Amer. Abstr. Prog.*, 23(5), 87, 1991.
- Smith, D.G. and T.G. Fisher, Glacial Lake Agassiz: the northwestern outlet and paleoflood, *Geology*, 21, 9-12, 1993.
- Snow, D.T., Landslide of Cerro Condor-Seneca. Department of Ayacucho, Peru, in *Geol. Soc. Amer. Eng. Geol. Case Histories, no. 5*, pp. 1-6, 1964.
- Stedinger, J.R., and T.A. Cohn, Flood frequency analysis with historical and paleoflood information, *Water Resour. Res.*, 22, 785-793, 1986.
- Teller, J.T., and L.H. Thorleifson, The Lake Agassiz-Lake Superior connection, in *Catastrophic Flooding*, edited by L. Mayer and D. Nash, pp. 121-138. Allen and Unwin, Boston, Massachusetts, 1987.
- Teller, J.T., and A.E. Kehew, Introduction to the late glacial history of large proglacial lakes and meltwater runoff along the Laurentide Ice Sheet, *Quat. Sci. Rev.*, 13, 795-799, 1994.
- Thorson, R.M., Late Quaternary paleofloods along the Porcupine River, Alaska: Implications for regional correlation, in *U.S. Geol. Surv. Circ. 1026*, pp. 51-54, 1989.
- U.S. Army Corps of Engineers, *Water Resource Development, Columbia River Basin*, 396 pp., U.S. Army Engineer Division, North Pacific, 1958.
- van der Leeden, F., F.L. Troise and D.K. Todd, *The Water Encyclopedia*, 808 pp., Lewis Publishers, Chasca, Minnesota, 1990.
- Vaughn, D., and D.W. Ash, Paleohydrology and geomorphology of selected reaches of the upper Wabash River, Indiana, *Geol. Soc. Amer. Abstr. Prog.*, 15(6), 711, 1983.
- Vörösmarty, C.J., B.M. Fekete, M. Meybeck and R.B. Lammers, Geomorphometric attributes of the global system of rivers at 30-minute spatial resolution, *J. Hydrol.*, 237, 17-39, 2000.
- Waananen, A.O., D.D. Harris and R.C. Williams, Floods of December 1964 and January 1965 in the far western states—Part 2. Streamflow and sediment data, *U.S. Geol. Surv. Water-Supply Pap. 1866-B*, 861 pp., 1970.
- Waitt, R.B., Great Holocene floods along Jökulsá á Fjöllum, North Iceland, in *Flood and Megaflood Processes, Recent and Ancient Examples, Intern. Assoc. Sedimentologists Spec. Publ.*, edited by I. P. Martini, V.R. Baker and G. Garzón, 2001 (in press).
- Walder, J.S. and J.E. Costa, Outburst floods from glacier-dammed lakes: The effect of mode of lake drainage on flood magnitude, *Earth Surf. Proc. Landf.*, 21, 701-723, 1996.
- Walder, J.S. and J.E. O'Connor, Methods for predicting peak discharge of floods caused by failure of natural and constructed earthen dams, *Water Resour. Res.*, 33, 2337-2348, 1997.
- Waythomas, C.R., J.S. Walder, R.G. McGimsey and C.A. Neal, A catastrophic flood caused by drainage of a caldera lake at Aniakchak volcano, Alaska, and implications for volcanic-hazards assessment, *Geol. Soc. Amer. Bull.*, 108, 861-871, 1996.
- Webb, R.H., J.E. O'Connor, and V.R. Baker, Paleohydrologic reconstruction of flood frequency on the Escalante River, south-central Utah, in *Flood Geomorphology*, edited by V.R. Baker, R.C. Kochel and P.C. Patton, pp. 403-418, John Wiley and Sons, New York, 1988.
- Webby, M.G. and D.N. Jennings, Analysis of dam break flood caused by failure of Tunawaea landslide dam, in *Proc. Intern. Conf. Hydraulics in Civil Eng.*, University of Queensland, Brisbane, Australia, pp. 163-168, 1994.
- Wolman, M.G., and J.E. Costa, Envelope curves for extreme flood events: Discussion, *J. Hydraul. Eng.*, 110, 77-78, 1984.
- World Meteorological Organization, *Manual for Estimation of Probable Maximum Precipitation, World Met. Org. Operational Hydrology Report No. 1 (second edition)*, 269 pp., Secretariat of the World Meteorological Organization, Geneva, Switzerland, 1986.

J.E. Costa, U.S. Geological Survey, 10615 S.E. Cherry Blossom Dr., Portland OR, 97216.

G.E. Grant, USDA Forest Service, Pacific Northwest Research Station, 3200 Jefferson Way, Corvallis, OR 97331

J.E. O'Connor, U.S. Geological Survey, 10615 S.E. Cherry Blossom Dr., Portland OR, 97216. (oconnor@usgs.gov)